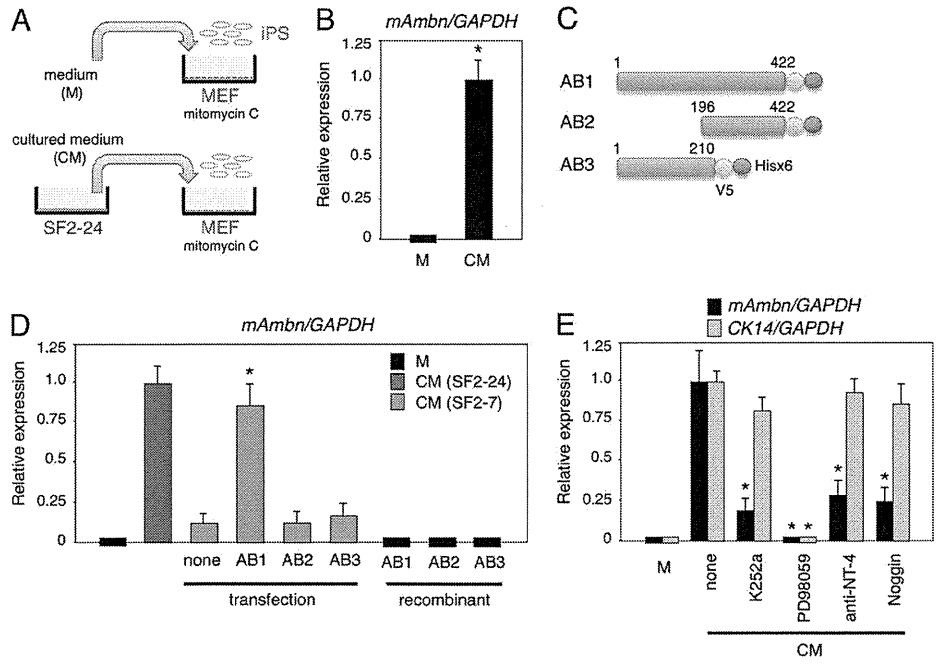

FIGURE 9. **Promotion of ameloblast induction of iPS cells using conditioned SF2-24 cells.** *A*, iPS cells were cultured on mitomycin C-treated MEFs in iPS cell culture medium supplemented with (*CM*) or without (*M*) conditioned medium from SF2-24 cells. *B*, expression of mouse Ambn gene in iPS cells cultured in iPS cell culture medium supplemented with (*CM*) or without (*M*) conditioned medium from SF2-24 cells. *C*, creation of Ambn deletions. All recombinant Ambn proteins have V5 and His tags at the C terminus. *D*, expression of mouse Ambn gene in iPS cells cultured in iPS cell culture medium supplemented with (*CM*) or without (*M*) condition medium from SF2-24 cells, recombinant Ambn-expressing SF2-7 cells or recombinant Ambn proteins. *, $p < 0.05$ (compared with non-transfected SF2-7 cells). *E*, expression of mouse Ambn and CK14 genes in iPS cells cultured in SF2-24 conditioned medium supplemented with K252a, PD98059, anti-NT-4, or Noggin. *, $p < 0.05$ (compared with CM only).

on dental epithelial cell differentiation by iPS cells, we analyzed the expressions of Ambn and CK14 in iPS cells cultured with SF2-24-conditioned medium in the presence of K252a (inhibitor of neurotrophic receptor Trk), PD98059 (MEK inhibitor), anti-NT-4 neutralizing antibody, or Noggin (BMP antagonist). K252a, PD98059, anti-NT-4, and Noggin each inhibited the expression of Ambn in iPS cells. Furthermore, CK14 expression in iPS cells was not inhibited by K252a, anti-NT-4, or Noggin (Fig. 9*E*). These results indicate that NT-4 and BMP signaling are important for differentiation into dental epithelial cells, but not CK14-positive epithelial cells.

DISCUSSION

Tooth development progresses through a number of stages, and the differentiation of dentin matrix-secreting odontoblasts and enamel matrix-producing ameloblasts results in formation of the crown. Ameloblasts and odontoblasts are central cell types involved in tooth development. In developing molars, restricted dental mesenchymal cells interact with the inner dental epithelium through the matrix and differentiate into odontoblasts. In the present study, we established an SP cell line from dental papilla mDP cells using cell sorting with Hoechst staining. SP cells are known to retain multipotency characteristics and can differentiate into various cell types, such as odontoblasts, osteoblasts, adipocytes, and neural cells. Our method for obtaining multipotent SP cells from a single cell line may be useful for development of novel therapeutic strategies that aim at regeneration of oral tissues.

Our co-culture assay of SP cells with dental epithelial cells showed that dental epithelial cells promote SP cell differentiation into DSPP-expressing cells via BMP2 and BMP4, which are secreted from dental epithelial cells (Fig. 5*B*, 5*D*, and 10*A*). Because BMP2 is not highly expressed in dental epithelium, BMP4 may be the dominant signaling regulator during odontoblast differentiation. In the early stages of tooth development, BMP4 is expressed in dental epithelium and induces the transcription factor Msx1 (30). The expression of DSPP is induced via the BMP signaling pathway in cooperation with Runx2, Dlx5, and Msx1 in undifferentiated mesenchymal cells (31). Previously, a bead soak assay of mandibular organ culture showed that BMP4 induced dental mesenchymal cell differentiation (32). Also, a transgenic approach revealed that inhibition of BMP4 by Noggin overexpression, driven by a keratin 14 promoter (K14-Noggin), resulted in the absence of all molars in the mandible. This indicates that BMP4 is essential for tooth bud formation by inducing dental mesenchymal cells (33). As demonstrated, in the present study odontoblastic differentiation of SP cells is completely disturbed by the blocking of BMP signaling. Thus, our finding strongly support the notion that BMP4 signaling is a key factor in induction of dental mesenchymal cells and their differentiation.

Differential synchronization between dental epithelial and mesenchymal cells has been observed during tooth development. Dental epithelial and mesenchymal cells are separated by a basement membrane, which is an essential regulator for epithelial-mesenchymal interaction (34). Both crown and root odontoblasts are induced by interactions with epithelial cells, such as those of the inner dental epithelium, epithelial rest, and epithelial diaphragm (35). Similar to *in vivo* situations, physical

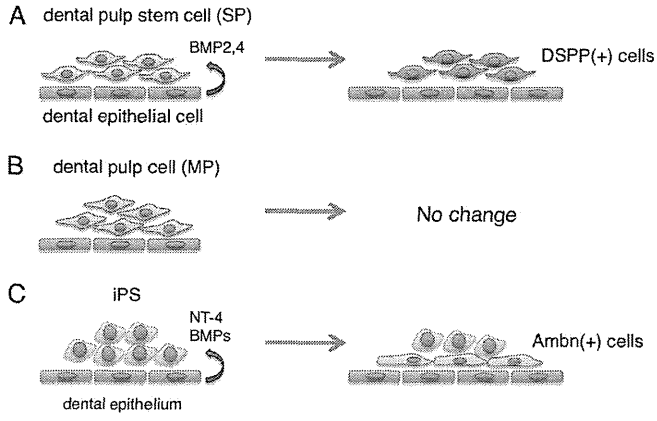

FIGURE 10. **Proposed models of odontogenic induction from dental mesenchymal stem cells and iPS cells by co-culturing with dental epithelial cells.** *A*, dental epithelial cells induce DSPP-expressing odontoblasts from SP cells. *B*, no odontogenic induction was observed in differentiated (*MP*) cells co-cultured with dental epithelial cells. *C*, dental epithelial cells induce Ambn-expressing ameloblasts from iPS cells.

cell attachment of dental epithelial cells was not required for odontogenic induction of SP cells in our experiments, indicating that soluble factors including BMPs are important for odontogenic induction by dental epithelial cells in culture. We also found that MP cells from dental papilla did not differentiate into DSPP-expressing cells, indicating that epithelial-mesenchymal interactions are important for cell fate determination of dental pulp stem cells, but not for differentiated dental pulp cells (Fig. 10, *A* and *B*). It was recently reported that Ambn protein, or a synthetic peptide based on the N-terminal region of the Ambn protein, induced osteoblastic cell differentiation (36). In addition to BMPs, Ambn may also be one of the factors involved in the odontogenic induction process, because the sharing of signaling pathways underlies the mechanism of odontoblastic and osteoblastic induction.

Ameloblasts secrete enamel-specific extracellular matrices including Ambn, which are lost upon tooth eruption. This makes it impossible to repair or replace damaged enamel in an erupted tooth. Therefore, identifying alternative sources of these cells becomes important. Bone marrow-derived cells can give rise to different types of epithelial cells. In mixed cultures with c-Kit+-enriched bone marrow cells, embryonic dental epithelial cells, and dental mesenchyme, bone marrow cells might be reprogrammed to give rise to ameloblast-like cells (37). Our strategy to create ameloblasts from mouse iPS cells may have direct application in tooth regeneration. We succeeded in establishing a co-culture system using cells derived from two different species, mouse iPS cells and rat derived enamel matrix secreting ameloblasts. This is the first demonstration of differentiation of iPS cells into ameloblasts through interactions with dental epithelium (Fig. 10*C*). However, a set of stem cell markers was continuously expressed in iPS cells after 7 days of co-culturing (Fig. 7*C*), indicating that a portion of the iPS cells had differentiated into enamel-secreting ameloblasts and some still retained stem cell potential. Thus, the efficacy of iPS cell differentiation into ameloblasts by enamel-secreting ameloblasts feeder cells must to be improved prior to for clinical application.

A number of factors are thought to give iPS cells the capacity for direct or indirect differentiation into ameloblasts. Possible direct effectors include gap junctions, intercellular binding molecules, adhesion factors, and extracellular matrices secreted by dental epithelium. Growth factors might also be involved, because conditioned medium from SF2-24 cells induced Ambn expression in iPS cells. Ambn is also a candidate factor for dental cell differentiation of iPS cells, as SF2 cells expressing low levels of Ambn did not induce differentiation of iPS cells. Furthermore, overexpression of full-length Ambn in cells expressing low levels of Ambn induced iPS cells into ameloblast-like differentiation (Fig. 9*D*). Ambn has diverse functions in various cellular physiologies, such as cell growth, differentiation, cell polarization, and attachment, though the detailed mechanisms of Ambn signaling require additional investigation. Ambn-null mice display severe enamel hypoplasia due to impaired dental epithelial cell proliferation, polarization, and differentiation into ameloblasts, as well as loss of cell attachment activity with immature enamel matrix (2). These results suggest that Ambn, especially full-length, is necessary for both *in vivo* and *in vitro* ameloblast differentiation.

There were differences in cell lineage determination of the dental pulp stem cells and iPS cells when co-cultured with dental epithelial cells. RT-PCR analysis showed that co-culturing induced SP cells to form odontoblastic cells, whereas iPS cells were induced to form ameloblastic cells. In addition, the expression of Brachyury, a mesodermal marker, in iPS cells was down-regulated by co-culturing with SF2-24 cells (Fig. 7*C*). Conversely, expressions of the epithelial markers p63 and CK14, as well as the dental epithelial marker epiprofin/Sp6 were up-regulated (Fig. 7*C*, supplemental Fig. S5) (28). These results suggest that the cell lineage of the iPS cells in our co-culturing system was effectively guided into an epithelial cell lineage. It has been reported that the default cell lineage of ES cells is the ectodermal cells, except when cultured in the presence of BMP antagonists (38, 39). Because BMPs promote ectodermal differentiation of ES cells, the expression of BMP observed in SF2 cells (Fig. 5*D*) may also contribute to dental epithelial cell differentiation of iPS cells. A previous our reported that NT-4 induced Ambn expression in dental epithelium, while NT-4 knock-out mice showed delayed expression of enamel matrices in the early stage of ameloblast differentiation (29). In the present study, the presence of the anti-NT-4 neutralizing antibody or Noggin in conditioned medium from SF2-24 cells inhibited Ambn expression, but not that of CK14 (Fig. 9*E*). On the other hand, SP cells strongly expressed the endogenous Sox2 protein, one of the reprogramming factors involved in generation of iPS cells (data not shown). Recently, iPS cells were generated from human dental pulp cells with a high level of efficiency in comparison to dermal fibroblasts, possibly due to a high expression level of Sox2 in dental pulp stem cells. However, additional reprogramming factors are required for creation of iPS cells from dental pulp cells. Thus, SP cells themselves did not have the same degree of multipotency as seen with ES and iPS cells. SP cells are considered to be mesenchymal stem cells that originate from dental pulp cells, which are derived from cranial neural crest cells. Neural crest cells can differentiate into several different cell lineages, such as neuron, glia, melanocyte,

osteoblast, chondrocyte, and odontoblast cells (40, 41). We believe that SP cells are not able to gain multipotency beyond the potential of neural crest cells. Thus, SP cells preserve some degree of multipotency that is different in an undifferentiated state as compared with ES and iPS cells. In co-cultures with SF2-24 cells, SP cells did not differentiate into ameloblasts, whereas iPS cells did (Fig. 10). Comparative analysis between SP and iPS cells is essential to clarify the mechanisms involved in directional cell fate determination.

In this study, we sought to clarify the role of dental epithelium and stem cell interactions by culturing rat dental epithelium with mouse iPS cells and SP cells. Rodent incisors grow throughout the lifespan of the animal by maintaining stem cells in the cervical loop, located at the end of incisor. A dental epithelial cell niche also exists in the cervical loop of the incisor. Analysis of gene knock-out mice for epiprofin/Sp6, an essential transcription factor for dental epithelial cell differentiation and enamel formation, has revealed that supernumerary teeth are formed by interactions between dental mesenchyme and undifferentiated dental epithelium (4, 42). In addition, those studies showed continuous signals from dental epithelial cells of mutant mice induced the continued differentiation of dental mesenchymal cells into odontoblasts (4, 42). Together these findings suggest that dental epithelial cells can induce dental mesenchymal cells to differentiate into odontoblasts. Therefore, rat dental epithelial cells may provide an *in vitro* niche environment for surrounding mouse iPS cells and SP cells. Elucidation of the mechanism of cell fate determination by dental epithelial cells may facilitate development of novel therapeutic approaches for regenerative dentistry.

REFERENCES

1. Thesleff, I. (2003) Epithelial-mesenchymal signaling regulating tooth morphogenesis. *J. Cell Sci.* **116,** 1647–1648
2. Fukumoto, S., Kiba, T., Hall, B., Iehara, N., Nakamura, T., Longenecker, G., Krebsbach, P. H., Nanci, A., Kulkarni, A. B., and Yamada, Y. (2004) Ameloblastin is a cell adhesion molecule required for maintaining the differentiation state of ameloblasts. *J. Cell Biol.* **167,** 973–983
3. Yuasa, K., Fukumoto, S., Kamasaki, Y., Yamada, A., Fukumoto, E., Kanaoka, K., Saito, K., Harada, H., Arikawa-Hirasawa, E., Miyagoe-Suzuki, Y., Takeda, S., Okamoto, K., Kato, Y., and Fujiwara, T. (2004) Laminin $\alpha 2$ is essential for odontoblast differentiation regulating dentin sialoprotein expression. *J. Biol. Chem.* **279,** 10286–10292
4. Nakamura, T., de Vega, S., Fukumoto, S., Jimenez, L., Unda, F., and Yamada, Y. (2008) Transcription factor epiprofin is essential for tooth morphogenesis by regulating epithelial cell fate and tooth number. *J. Biol. Chem.* **283,** 4825–4833
5. Fisher, L. W., and Fedarko, N. S. (2003) Six genes expressed in bones and teeth encode the current members of the SIBLING family of proteins. *Connect Tissue Res.* **44,** Suppl. 1, 33–40
6. Takahashi, K., Tanabe, K., Ohnuki, M., Narita, M., Ichisaka, T., Tomoda, K., and Yamanaka, S. (2007) Induction of pluripotent stem cells from adult human fibroblasts by defined factors. *Cell* **131,** 861–872
7. Lewitzky, M., and Yamanaka, S. (2007) Reprogramming somatic cells towards pluripotency by defined factors. *Curr. Opin. Biotechnol.* **18,** 467–473
8. Xu, D., Alipio, Z., Fink, L. M., Adcock, D. M., Yang, J., Ward, D. C., and Ma, Y. (2009) Phenotypic correction of murine hemophilia A using an iPS cell-based therapy. *Proc. Natl. Acad. Sci. U.S.A.* **106,** 808–813
9. Hanna, J., Wernig, M., Markoulaki, S., Sun, C. W., Meissner, A., Cassady, J. P., Beard, C., Brambrink, T., Wu, L. C., Townes, T. M., and Jaenisch, R. (2007) Treatment of sickle cell anemia mouse model with iPS cells generated from autologous skin. *Science* **318,** 1920–1923
10. Soldner, F., Hockemeyer, D., Beard, C., Gao, Q., Bell, G. W., Cook, E. G., Hargus, G., Blak, A., Cooper, O., Mitalipova, M., Isacson, O., and Jaenisch, R. (2009) Parkinson disease patient-derived induced pluripotent stem cells free of viral reprogramming factors. *Cell* **136,** 964–977
11. Okita, K., Ichisaka, T., and Yamanaka, S. (2007) Generation of germline-competent induced pluripotent stem cells. *Nature* **448,** 313–317
12. So, K. H., Han, Y. J., Park, H. Y., Kim, J. G., Sung, D. J., Bae, Y. M., Yang, B. C., Park, S. B., Chang, S. K., Kim, E. Y., and Park, S. P. (2010) *Int. J. Cardiol.* **153,** 277–285
13. Yoshida, Y., and Yamanaka, S. (2011) *J. Mol. Cell Cardiol.* **50,** 327–332
14. Miura, M., Gronthos, S., Zhao, M., Lu, B., Fisher, L. W., Robey, P. G., and Shi, S. (2003) SHED: stem cells from human exfoliated deciduous teeth. *Proc. Natl. Acad. Sci. U.S.A.* **100,** 5807–5812
15. Gronthos, S., Mankani, M., Brahim, J., Robey, P. G., and Shi, S. (2000) Postnatal human dental pulp stem cells (DPSCs) *in vitro* and *in vivo*. *Proc. Natl. Acad. Sci. U.S.A.* **97,** 13625–13630
16. Shi, S., Bartold, P. M., Miura, M., Seo, B. M., Robey, P. G., and Gronthos, S. (2005) The efficacy of mesenchymal stem cells to regenerate and repair dental structures. *Orthod. Craniofac Res.* **8,** 191–199
17. Goodell, M. A., Brose, K., Paradis, G., Conner, A. S., and Mulligan, R. C. (1996) Isolation and functional properties of murine hematopoietic stem cells that are replicating *in vivo*. *J. Exp. Med.* **183,** 1797–1806
18. Zhou, S., Schuetz, J. D., Bunting, K. D., Colapietro, A. M., Sampath, J., Morris, J. J., Lagutina, I., Grosveld, G. C., Osawa, M., Nakauchi, H., and Sorrentino, B. P. (2001) The ABC transporter Bcrp1/ABCG2 is expressed in a wide variety of stem cells and is a molecular determinant of the side-population phenotype. *Nat. Med.* **7,** 1028–1034
19. Li, L., Kwon, H. J., Harada, H., Ohshima, H., Cho, S. W., and Jung, H. S. (2011) Expression patterns of ABCG2, Bmi-1, Oct-3/4, and Yap in the developing mouse incisor. *Gene Expr. Patterns* **11,** 163–170
20. Nam, H., and Lee, G. (2009) Identification of novel epithelial stem cell-like cells in human deciduous dental pulp. *Biochem. Biophys. Res. Commun.* **386,** 135–139
21. Yan, X., Qin, H., Qu, C., Tuan, R. S., Shi, S., and Huang, G. T. (2010) iPS cells reprogrammed from human mesenchymal-like stem/progenitor cells of dental tissue origin. *Stem. Cells Dev.* **19,** 469–480
22. Yokoi, T., Saito, M., Kiyono, T., Iseki, S., Kosaka, K., Nishida, E., Tsubakimoto, T., Harada, H., Eto, K., Noguchi, T., and Teranaka, T. (2007) Establishment of immortalized dental follicle cells for generating periodontal ligament *in vivo*. *Cell Tissue Res.* **327,** 301–311
23. Klotz, O. (1905) Studies upon calcareous degeneration: I. The process of pathological calcification. *J. Exp. Med.* **7,** 633–674
24. Sonoda, A., Iwamoto, T., Nakamura, T., Fukumoto, E., Yoshizaki, K., Yamada, A., Arakaki, M., Harada, H., Nonaka, K., Nakamura, S., Yamada, Y., and Fukumoto, S. (2009) Critical role of heparin binding domains of ameloblastin for dental epithelium cell adhesion and ameloblastoma proliferation. *J. Biol. Chem.* **284,** 27176–27184
25. Chen, S., Gu, T. T., Sreenath, T., Kulkarni, A. B., Karsenty, G., and MacDougall, M. (2002) Spatial expression of Cbfa1/Runx2 isoforms in teeth and characterization of binding sites in the *DSPP* gene. *Connect. Tissue Res.* **43,** 338–344
26. Cukierman, E., Pankov, R., Stevens, D. R., and Yamada, K. M. (2001) Taking cell-matrix adhesions to the third dimension. *Science* **294,** 1708–1712
27. Nakashima, M. (1994) Induction of dentin formation on canine amputated pulp by recombinant human bone morphogenetic proteins (BMP)-2 and -4. *J. Dent. Res.* **73,** 1515–1522
28. Nakamura, T., Unda, F., de-Vega, S., Vilaxa, A., Fukumoto, S., Yamada, K. M., and Yamada, Y. (2004) The Krüppel-like factor epiprofin is expressed by epithelium of developing teeth, hair follicles, and limb buds and promotes cell proliferation. *J. Biol. Chem.* **279,** 626–634
29. Yoshizaki, K., Yamamoto, S., Yamada, A., Yuasa, K., Iwamoto, T., Fukumoto, E., Harada, H., Saito, M., Nakasima, A., Nonaka, K., Yamada, Y., and Fukumoto, S. (2008) Neurotrophic factor neurotrophin-4 regulates ameloblastin expression via full-length TrkB. *J. Biol. Chem.* **283,** 3385–3391
30. Chen, Y., Bei, M., Woo, I., Satokata, I., and Maas, R. (1996) Msx1 controls inductive signaling in mammalian tooth morphogenesis. *Development* **122,** 3035–3044

31. Cho, Y. D., Yoon, W. J., Woo, K. M., Baek, J. H., Park, J. C., and Ryoo, H. M. (2010) The canonical BMP signaling pathway plays a crucial part in stimulation of dentin sialophosphoprotein expression by BMP-2. *J. Biol. Chem.* **285,** 36369–36376
32. Vainio, S., Karavanova, I., Jowett, A., and Thesleff, I. (1993) Identification of BMP-4 as a signal mediating secondary induction between epithelial and mesenchymal tissues during early tooth development. *Cell* **75,** 45–58
33. Plikus, M. V., Zeichner-David, M., Mayer, J. A., Reyna, J., Bringas, P., Thewissen, J. G., Snead, M. L., Chai, Y., and Chuong, C. M. (2005) Morphoregulation of teeth: modulating the number, size, shape and differentiation by tuning Bmp activity. *Evol. Dev.* **7,** 440–457
34. Thesleff, I., and Hurmerinta, K. (1981) Tissue interactions in tooth development. *Differentiation* **18,** 75–88
35. Ten Cate, A. R. (1996) The role of epithelium in the development, structure and function of the tissues of tooth support. *Oral Dis.* **2,** 55–62
36. Iizuka, S., Kudo, Y., Yoshida, M., Tsunematsu, T., Yoshiko, Y., Uchida, T., Ogawa, I., Miyauchi, M., and Takata, T. (2011) Ameloblastin regulates osteogenic differentiation by inhibiting Src kinase via cross talk between integrin β1 and CD63. *Mol. Cell Biol.* **31,** 783–792
37. Hu, B., Unda, F., Bopp-Kuchler, S., Jimenez, L., Wang, X. J., Haïkel, Y., Wang, S. L., and Lesot, H. (2006) Bone marrow cells can give rise to ameloblast-like cells. *J. Dent. Res.* **85,** 416–421
38. Chang, C., and Hemmati-Brivanlou, A. (1998) Cell fate determination in embryonic ectoderm. *J. Neurobiol.* **36,** 128–151
39. Muñoz-Sanjuan, I., and Brivanlou, A. H. (2002) Neural induction, the default model and embryonic stem cells. *Nat. Rev. Neurosci.* **3,** 271–280
40. Baroffio, A., Dupin, E., and Le Douarin, N. M. (1991) Common precursors for neural and mesectodermal derivatives in the cephalic neural crest. *Development* **112,** 301–305
41. Sieber-Blum, M., and Cohen, A. M. (1980) Clonal analysis of quail neural crest cells: they are pluripotent and differentiate *in vitro* in the absence of noncrest cells. *Dev. Biol.* **80,** 96–106
42. Nakamura, T., Fukumoto, S., and Yamada, Y. (2011) Review: diverse function of epiprofin in tooth development. *J. Oral Biosci.* **53,** 22–30

THE JOURNAL OF BIOLOGICAL CHEMISTRY VOL. 287, NO. 15, pp. 12217–12229, April 6, 2012

Roles of Heparan Sulfate Sulfation in Dentinogenesis*

Received for publication, December 13, 2011, and in revised form, January 29, 2012 Published, JBC Papers in Press, February 20, 2012, DOI 10.1074/jbc.M111.332924

Satoru Hayano[‡], Hiroshi Kurosaka[‡], Takeshi Yanagita[‡], Ina Kalus[§], Fabian Milz[§], Yoshihito Ishihara[‡], Md. Nurul Islam[‡], Noriaki Kawanabe[‡], Masahiro Saito[¶], Hiroshi Kamioka[‡], Taiji Adachi[‖], Thomas Dierks[§], and Takashi Yamashiro[‡1]

From the [‡]Department of Orthodontics, Okayama University Graduate School of Medicine, Dentistry, and Pharmaceutical Sciences, Okayama University, Okayama 700-8525, Japan, the [§]Department of Chemistry, Biochemistry I, Bielefeld University, Bielefeld 33501, Germany, the [¶]Faculty of Industrial Science and Technology, Tokyo University of Science, Tokyo 162-8601, Japan, and the [‖]Department of Biomechanics, Research Center for Nano Medical Engineering, Institute for Frontier Medical Sciences, Kyoto University, Kyoto 606-8507, Japan

Background: Cell surface heparan sulfate is an essential regulator of cell signaling.
Results: Sulf 6-*O*-endosulfatase deficiency results in degenerative phenotypes, and HSPG sulfation status induces Wnt10a-mediated activation of odontoblast differentiation.
Conclusion: Sulf-mediated desulfation is an important modification for the activation of the Wnt signaling in odontoblasts.
Significance: This is the first molecular evidence for the functional roles of HSPG sulfation in dentin formation.

Cell surface heparan sulfate (HS) is an essential regulator of cell signaling and development. HS traps signaling molecules, like Wnt in the glycosaminoglycan side chains of HS proteoglycans (HSPGs), and regulates their functions. Endosulfatases Sulf1 and Sulf2 are secreted at the cell surface to selectively remove 6-*O*-sulfate groups from HSPGs, thereby modifying the affinity of cell surface HSPGs for its ligands. This study provides molecular evidence for the functional roles of HSPG sulfation and desulfation in dentinogenesis. We show that odontogenic cells are highly sulfated on the cell surface and become desulfated during their differentiation to odontoblasts, which produce tooth dentin. *Sulf1/Sulf2* double null mutant mice exhibit a thin dentin matrix and short roots combined with reduced expression of dentin sialophosphoprotein (*Dspp*) mRNA, encoding a dentin-specific extracellular matrix precursor protein, whereas single *Sulf* mutants do not show such defective phenotypes. In odontoblast cell lines, *Dspp* mRNA expression is potentiated by the activation of the Wnt canonical signaling pathway. In addition, pharmacological interference with HS sulfation promotes *Dspp* mRNA expression through activation of Wnt signaling. On the contrary, the silencing of *Sulf* suppresses the Wnt signaling pathway and subsequently *Dspp* mRNA expression. We also show that Wnt10a protein binds to cell surface HSPGs in odontoblasts, and interference with HS sulfation decreases the binding affinity of Wnt10a for HSPGs, which facilitates the binding of Wnt10a to its receptor and potentiates the Wnt signaling pathway, thereby up-regulating *Dspp* mRNA expression. These results demonstrate that Sulf-mediated desulfation of cellular HSPGs is an important modification that is critical for the activation of the Wnt signaling in odontoblasts and for production of the dentin matrix.

Sugar chain protein modification is a post-translational modification of genetic information, and the resultant sugar chain heterogeneity is associated with many diseases, immunity, and development. Heparan sulfate (HS)[2] is a member of the glycosaminoglycan (GAG) family of polysaccharides, which attaches to core proteins to form proteoglycans and is ubiquitously present on the cell surface and in the extracellular matrix (1). It is also an essential regulator of cell signaling and development. HS traps many different proteins on the cell surface and basement membrane and regulates their functions (2, 3). There is considerable interest in the structural variability generated by a series of modifications within HS, which are responsible for the binding and regulation of specific HS-interacting proteins (4, 5). Such HS modifications, in particular in the form of its sulfation patterns, result in structural and functional heterogeneity, which are controlled in a tissue-specific and developmental manner (6). Here the specific and inhomogenous sulfation of the HS disaccharide building blocks (*i.e.* at the *N*-, 3-*O*-, and 6-*O*-position of glucosamine and the 2-*O*- position of hexuronic acid) (7) translates into dynamic docking sites for various ligands, among them important signaling molecules, such as FGF and Wnt.

Dentin is the mineralized portion of tooth tissue, and it is produced by odontoblasts differentiating from dental papilla mesenchymal cells. Dentinogenesis is regulated by sequential and reciprocal interactions with the dental epithelium mediated by epithelial-mesenchymal interactions, which direct both morphogenesis and differentiation (8–10). Odontoblasts are characteristically columnar polarized cells, and this cytological polarization specifically occurs in a single layer adjacent to the inner dental epithelium (11). Dentin sialophosphoprotein (Dspp) is a phosphorylated parent protein that is cleaved post-translationally into two dentin non-collagenous proteins: dentin sialoprotein (Dsp) and dentin phosphoprotein (Dpp) (12). *In*

* This work was supported by grants-in-aid for scientific research program from the Japan Society for the Promotion of Science (to T. Y.).
[1] To whom correspondence should be addressed. Tel.: 81-86-235-6694; Fax: 81-86-235-6694; E-mail: yamataka@md.okayama-u.ac.jp.

[2] The abbreviations used are: HS, heparan sulfate; GAG, glycosaminoglycan; HSPG, HS proteoglycan; β-D-xyloside; miRNA, microRNA; CT, computed tomography; E*n*, embryonic day *n*; P*n*, postnatal day *n*.

situ hybridization and other experimental analyses have shown that *Dspp* is predominantly expressed in odontoblasts, transiently expressed in preameloblasts, and expressed at low levels in bone (13, 14). This suggests that the functional role of Dspp mainly involves tooth formation and mineralization. In humans, several mutations in *DSPP* have been identified in patients with dentinogenesis imperfecta, which is an autosomal dominant disorder of the tooth that specifically affects dentin biomineralization (15–18). A similar phenotype is found in *Dspp* null mutant mice, which disrupts dentin mineralization without affecting bone (19). Hence, it is established that Dspp plays a specific and crucial role in the formation of mineralized dentin.

Wnt genes encode a large family of secreted signaling proteins that specify various cell lineage pathways during development. Wnt proteins are now recognized as one of the major families of developmentally important signaling molecules (20). Among the functions performed by Wnt proteins are embryonic induction, the generation of cell polarity, and the specification of cell fate. The canonical Wnt pathway involves inhibition of the β-catenin degradation complex, allowing its interaction with the nuclear transcription factors LEF and TCF and the regulation of target gene expression (21). In early tooth development, various *Wnt* genes are expressed from the bud stage to the early bell stage (22). A recent study revealed that *TOPGAL* and *Axin2* reporter activity are high in the odontoblast layer (23, 24), suggesting that dentinogenesis is associated with the activation of the canonical Wnt signaling pathway. These findings are in line with the human tooth phenotypes observed after the heterozygotic loss of *Axin2* function, which causes tooth agenesis and/or hypodontia (25). Among the numerous *Wnt* genes that are expressed in developing tooth germs, *Wnt10a* is specifically expressed in odontoblasts. Interestingly, the forced expression of *Wnt10a* induced *Dspp* expression when the transfected cells were cultured on Matrigel (26), indicating that *Wnt10a* is an upstream gene involved in *Dspp* expression. In addition, human *WNT10A* mutations were reported to be associated with hypodontia (27, 28). These findings strongly suggest that the Wnt10a-induced canonical Wnt pathway is involved in dentinogenesis, at least in part, by directly activating *Dspp* expression, although there is no direct *in vivo* or *in vitro* evidence to support this.

The Sulf proteins Sulf1 and Sulf2 were identified as a family of extracellular glucosamine-6-sulfatases that remove the sulfate groups from the 6-*O*-position of *N*-acetylglucosamine (29, 30). Both Sulf1 and Sulf2 are endosulfatases that act extracellularly and generate structural heterogeneity along HS chains by modifying the sulfation pattern of HS postsynthetically. *Sulf1/Sulf2* double null mutant mice show numerous distinct phenotypes (31–37). In skeletal structures, malformations, including reduced bone length, premature vertebrae ossification, and fusion of sternebrae and tail vertebrae, are observed (35). Due to their activity, the Sulfs control HS proteoglycans (HSPGs) functioning as coreceptors for the signaling activities of multiple developmental ligands (32). In particular, Sulf1 activity has been shown to decrease the affinity of HS toward the Wnt ligand and promote the binding of Wnt to its cognate receptor Frizzled, thereby acting as a positive regulator of Wnt signaling (38). From these findings, together with those of our previous study (26), we hypothesized that Wnt ligands, especially Wnt10a, can be captured by cell surface or basement membrane extracellular matrix molecules to control the differentiation of pulp cells into odontoblasts and that such regulation of Wnt signaling is modulated by the Sulf enzymes.

This study presents the first molecular evidence for the functional roles of HSPG sulfation and desulfation in dentin formation. Here, we demonstrate that the desulfation of odontogenic cells progresses with differentiation and that the loss of the endosulfatases Sulf1 and Sulf2 results in defective dentin phenotypes. In particular, we show that the cell surface sulfation of HSPGs affects the Wnt canonical signaling pathway and consequently regulates *Dspp* expression in odontogenic cells. We also show that the binding affinity of HS for Wnt10a is directly dependent on its 6-*O*-sulfation status.

EXPERIMENTAL PROCEDURES

Animals—Sulf1 and *Sulf2* mutant embryos and postnatal mice were used in this study. *Sulf1* and *Sulf2* knock-out mice were generated by the insertion of a neomycin resistance cassette into exon 2 of the murine *Sulf1* gene and exon 1 of the murine *Sulf2* gene, as described previously (37). Control mouse fetuses were also obtained from the ICR strain. The control group consisted of control or single-transgenic animals from the same litter. Animal experiments were performed under the research protocol approved by the Animal Research Committee at Bielefeld University and Okayama University.

Cell Culture—The mDP odontoblast-like cell line, which was derived from the embryonic mouse mesenchyme (39), was used in this study. The mDP cells were maintained in Dulbecco's modified Eagle's medium (DMEM) supplemented with 10% fetal bovine serum (FBS) and 1% penicillin and streptomycin at 37 °C in a humidified atmosphere containing 5% CO_2. The cells were subcultured every 3–4 days, and 0.05% (w/v) EDTA was used to detach the cells from the culture dish. These cells were used for the real-time PCR experiments.

Sodium chlorate is a reversible inhibitor of glycosaminoglycan sulfation. mDP cells were treated to pharmacologically remove sulfated residues from their cell surface HSPGs (40). The chlorate-treated cultures were incubated with 50 mM sodium chlorate for 72 h before being processed for immunocytochemistry and real-time RT-PCR analysis.

Lithium chloride (LiCl) is an inhibitor of glycogen synthase kinase-3 and mimics Wnt signaling by inhibiting glycogen synthase kinase-3 activity (41). mDP cell lines were treated with 50 mM LiCl for 5 days before being processed for immunocytochemistry and real-time RT-PCR analysis.

The cells were also incubated with 1 mM 4-nitrophenyl-β-D-xylopyranoside (β-D-xyloside) (Sigma) for 72 h. β-D-Xyloside is a primer of GAG chain synthesis and inhibitor of proteoglycan assembly (42, 43). Consequently, at 1 mM β-D-xyloside, HSs without core proteins are supposed to be released from the cells and may form a complex with Wnts in the conditioned medium. In the present study, we also confirmed that 1 mM β-D-xyloside does not affect the proliferation of cells or type I collagen synthesis in odontoblast cell lines (data not shown). Therefore, we can rule out a toxic effect of β-D-xyloside. Fur-

ther, mDP cells were incubated for 120 h with 5 units/ml heparin (Fuso Pharma, Osaka, Japan), which directly binds free Wnt proteins released into the culture medium.

Microcomputed Tomography (Micro-CT)—Three-dimensional images of tooth structure were analyzed using an inspeXio SMX-90CT Microfocus x-ray CT system, (Shimadzu, Kyoto, Japan). Briefly, image acquisition was performed at 90 kV and 110 mA. The resultant images were processed by the three-dimensional reconstruction software VG Studio MAX 2.0 (Volume Graphics, Heidelberg, Germany). The image reconstruction was carried out using appropriate cross-sections at a spatial resolution of 17 μm and was used to perform comparative measurements of tooth morphology.

The following parameters were defined: root length, distance between the apex and the cemento-enamel junction along the root canal for the mesial root of the first lower molar; crown length, anteroposterior distance between the mesial marginal ridge and the distal marginal ridge along the occlusal plane; dentin thickness, mean of the mesial and distal dentin thickness at the level of the cement-enamel junction; enamel thickness, mean of the mesial and distal enamel thickness at the midlevel of crown height.

Tissue Preparation and Histology—Embryonic day 16.5 (E16.5) and postnatal day 0 (P0), P1, P7, and P28 heads were fixed in 4% paraformaldehyde or tissue fixative (Genostaff, Tokyo, Japan) at 4 °C overnight. P7 and P28 heads were decalcified in 12.5% EDTA for 3 weeks. Then they were dehydrated, embedded in paraffin, and serially sectioned at 7 or 6 μm for hematoxylin and eosin staining and *in situ* hybridization. Frozen cross-sections (10 μm) were also prepared for *in situ* hybridization and immunohistochemistry. Those embryos were fixed in 4% paraformaldehyde at 4 °C overnight, incubated in 30% sucrose/PBS at 4 °C overnight, embedded in OCT compound (Sakura Finetek, Tokyo, Japan), and serially sectioned at 10 μm.

Predentin thickness was measured in frontal sections of P0 control and *Sulf1*/*Sulf2* double null mutant lower molars. The maximum thickness of the predentin beneath the mesial cusps was measured in serial sections from each group.

Immunohistochemistry and in Situ Hybridization—*In situ* hybridization using digoxigenin-labeled RNA probes was performed as described previously (44). Mouse *Sulf1 and Sulf2* probes were generated from a 461-bp *Sulf1* fragment spanning the region between 124 and 584 in accession number AY101178 and a 459-bp *Sulf2* fragment spanning the region between 3056 and 3514 in accession number AY101178. The preparation of *Wnt10a*, *Dspp*, and *Axin2* RNA probes has been described previously (23, 26).

Cell proliferation was assessed by 5′-bromo-2-deoxyuridine (BrdU) labeling of dividing cells in the tooth germs of *Sulf1* and *Sulf2* mutants. E18.5 pregnant mice were intraperitoneally injected with 1.5 ml/100 g body weight of BrdU solution (Sigma) and killed after 2 h. BrdU staining was carried out in paraffin sections using a BrdU staining kit according to the manufacturer's instructions (Zymed Laboratories Inc., South San Francisco, CA). Cell proliferation indices were determined by counting the BrdU-positive and -negative cells in defined areas of the cervical loop epithelium and mesenchyme.

Immunohistochemistry was performed on frozen sections of developing tooth germs and mDP cells. The sulfated HS distribution was visualized using 10E4 antibody (1:100; Seikagaku, Tokyo, Japan). HS distribution was visualized using the 3G10 antibody (1:100; Seikagaku). 3G10 identifies a neoepitope generated by heparinase III digestion of HS. Sections were pretreated with heparinase III (400 milliunits/ml for 2 h) immediately before immunohistochemistry.

Immunohistochemistry for Wnt10a (ab62051, Abcam (Cambridge, UK)) was also performed using mDP cells. Secondary antibodies conjugated with the appropriate fluorochrome, Cy™3-conjugated AffiniPure goat anti-mouse IgG + IgM antibody (1:500; Seikagaku) were used.

Immunoreactivity to 10E4, 3G10, and Wnt10a was visualized with a FLUOVIEW FV500 confocal laser-scanning microscopy system (Olympus, Tokyo, Japan) equipped for differential interference contrast microscopy. The confocal laser-scanning microscopy system was coupled to an upright microscope (IX-71, Olympus) with a ×60 (numerical aperture = 1.4) oil immersion objective lens.

RNA Extraction and Real-time RT-PCR Analysis—Total RNA was extracted from the mDP cells using Isogen (Nippon Gene, Tokyo, Japan), according to the manufacturer's protocol. Mandibular fragments containing tooth germs were also isolated from P0 transgenic and wild-type mouse pups and fixed overnight in buffered 4% paraformaldehyde. First molar tooth germs of the mandible were dissected in 0.1 M phosphate buffer (pH 7.4) under a stereomicroscope. Total RNA was isolated from formalin-fixed tooth germ using a RecoverAll total nucleic acid isolation kit (Ambion, Austin, TX) according to the manufacturer's protocol. Total RNA (500 ng) was reverse-transcribed to cDNA using oligo(dT)$_{20}$ primer (Takara, Shiga, Japan). For real-time RT-PCR analysis, the cDNA were amplified with Blend-Taq Plus (Toyobo, Osaka, Japan) and a regular thermal cycler. Quantitative real-time PCR was performed in duplicate for four independent sets of samples. The relative quantity of transcripts was determined using a standard curve and normalized in comparison with the expression of *Gapdh* mRNA. The sets of synthetic primers used for the amplification are as follows: mouse glyceraldehyde-3-phosphate dehydrogenase gene (*Gapdh*), 5′-GTCCCGTAGACAAAATGGTG-3′ (sense) and 5′-CAATGAAGGGGTCGTTGATG-3′ (antisense); mouse *Dspp*, 5′-AGCCGTGGAGATGCTTCTTA-3′ (sense) and 5′-TCACTCTCGCTGTCACCATC-3′ (antisense); mouse *Axin2*, 5′-CCTTGCCAAAACGGAATG-3′ (sense) and 5′-TTTCGTGGCTGTTGCGTA-3′ (antisense). Each PCR was carried out and analyzed as described previously (45). Each amplification reaction was performed and checked to ensure the absence of nonspecific PCR products by melting curve analysis using a LightCycler™ system (Roche Applied Science). The relative cDNA copy numbers were computed using data from serial dilutions of representative samples for each target gene. The same pools of rat E17 head cDNA and mouse P0 tibia cDNA were used as calibrators.

Overexpression and Suppression of Sulf—For the overexpression of *Sulf1* and *Wnt10a*, the pLPCX-based (pCI-neo-based) *Sulf1*-RGS-His6 expression vector (46) and the pCMV-based

Wnt10a expression vector (26) were used, respectively. These vectors or empty vectors as a control, pMAX-GFP (Amaxa, Koeln, Germany), were transfected into mDP cells using the FuGENE 6 transfection reagent (Roche Applied Science) according to the manufacturer's protocols.

For the suppression of *Sulf2*, the BLOCK-iT Pol II miR RNAi expression vector (Invitrogen) was used to silence mouse *Sulf2*. Two different double-stranded oligonucleotide duplexes encoding the desired miRNA sequences were selected using online software (BLOCK-iT RNAi Designer, Invitrogen) and ligated into the expression vector. The sequences of the two selected oligonucleotide duplexes were as follows: first *Sulf2* miRNA, 5′-TGCTGAAAGCGGGAGTTCTTAAGTAGGTTTTGGCCACTGACTGACCTACTTAAACTCCCGCTTT-3′ (top sequence) and 5′-CCTGAAAGCGGGAGTTTAAGTAGGTCAGTCAGTGGCCAAAACCTACTTAAGAACTCCGCTTTC-3′ (bottom sequence); second *Sulf2* miRNA, 5′-TGCTGTTCTATGGCAGTCACATTCTTGTTTTGGCCACTGACTGACAAGAATGTCTGCCATAGAA-3′ (top sequence) and 5′-CCTGTTCTATGGCAGACATTCTTGTCAGTCAGTGGCCAAAACAAGAATGTGACTGCCATAGAAC-3′ (bottom sequence). Vectors containing the *Sulf2*-miRNA plasmid were transfected into mDP cells using FuGENE 6 according to the manufacturer's protocols.

Statistical Analysis—Data are shown as the mean ± S.D. Statistical significance was evaluated using the Mann-Whitney *U* test for group comparisons, and $p < 0.05$ was considered significant. Statistical analyses were performed using SPSS version 12.0 (SPSS Inc., Chicago, IL).

Affinity Chromatography—To investigate the affinity of Wnt10a toward HS, which had been either pretreated with active Sulf1 (termed HS-6S) or not (HS+6S), we used columns with immobilized HS-6S and HS+6S. Generation of these columns and characterization of their HS disaccharide composition has been described previously (47). Briefly, HS from porcine intestinal mucosa (Celsus Laboratories, Cincinnati, OH) was treated with purified, active Sulf1DHDC enzyme, reductively aminated, and covalently immobilized on a HiTrap NHS activated 1-ml column (GE Healthcare). Accordingly, immobilization of untreated HS was performed on a second HiTrap NHS column. On each column, after equilibration with buffer A (20 mM Tris, pH 7.4), 35 μl of Wnt10a-containing cell lysate (Origene Technologies, Rockville, MD) was loaded and subjected to chromatography by using an ÄKTA Explorer chromatography system. After washing with 2 ml of buffer A, bound Wnt10a was eluted using a linear 10-ml gradient from 0 to 100% buffer B (20 mM Tris, pH 7.4, 1.5 M NaCl). Fractions of 1 ml were collected, concentrated 20-fold by using a 500-μl Spin-X concentrator (Corning Glass, 10,000 molecular weight cut-off), and analyzed by Western blotting using a polyclonal anti-Wnt10a antibody (Abcam, Cambridge, MA).

RESULTS

Specific Heparan Sulfate Modification during Tooth Development—To investigate the role of the sulfation status of heparan sulfate in tooth development, we examined the temporospatial changes of heparan sulfate sulfation, as specifically recognized by the 10E4 antibody (48–50). At E16.5 (Fig. 1*A*), we

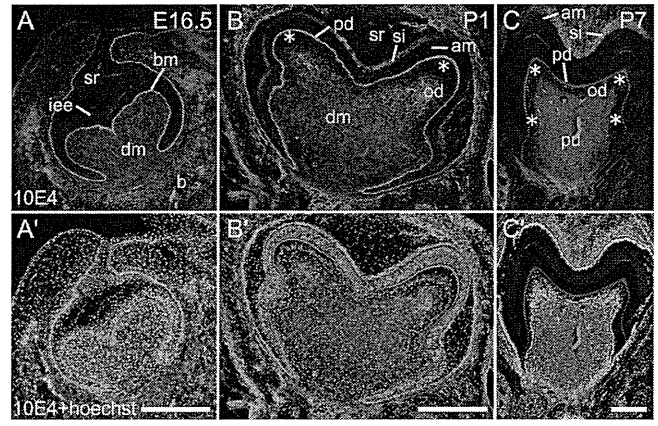

FIGURE 1. **Analysis of the sulfated HS distribution during tooth development at E16.5 (*A*), P1 (*B*), and P7 (*C*).** Immunofluorescent staining for 10E4 was visualized using the Cy™3-conjugated secondary antibody, which is shown in *red*. Nuclear staining with Hoechst is shown in blue (*A*′–*C*′). *A* and *A*′, 10E4 staining was ubiquitously present in the dental mesenchyme and the surrounding bones (*b*). The staining was intense in the basement membrane (*bm*) and reduced in the dental epithelium, including the inner enamel epithelium (*iee*) and the stellate reticulum (*sr*). *B* and *B*′, polarized and differentiated odontoblasts were observed in the mesenchyme underlying the future cusp region, and 10E4 staining was significantly reduced in these odontoblasts (*asterisks* in Fig. 1*B*), whereas 10E4 staining was retained in the dental mesenchyme (*dm*) of the future pulp. The 10E4 staining was significantly reduced in the differentiated ameloblasts (*am*), and intense 10E4 staining was present in the predentin (*pd*). This staining was continuous with that in the basement membrane (*bm*). *C* and *C*′, the 10E4 staining was almost completely absent from the odontoblasts (*od* and *asterisks*) and ameloblasts (*am*) but was intense in the dental pulp (*pu*). *si*, stratum intermedium; *Scale bars* (*A*′, *B*′, and *C*′), 200 μm.

observed ubiquitous 10E4 staining in both tooth germs, including the dental mesenchyme (*dm*) and the surrounding bones (*b*). The staining was reduced in the dental epithelium, including the inner enamel epithelium (*iee*) and the stellate reticulum (*sr*). In contrast, it was intense in the basement membrane (*bm*). At P1 (Fig. 1*B*), polarized and differentiated odontoblasts were observed in the mesenchyme underlying the future cusp regions, and 10E4 staining was significantly reduced in these odontoblasts (*asterisks* in Fig. 1*B*), whereas normal 10E4 staining was retained in the dental mesenchyme (*dm*) of the future pulp. In addition, 10E4 staining was significantly reduced in the differentiated ameloblasts (*am*). In contrast, 10E4 staining also labeled the basement membrane (*bm*), predentin (*pd*), and stratum intermedium (*si*). At P7 (Fig. 1*C*), 10E4 staining was almost completely abolished in the odontoblasts (*od*) (*asterisks* in Fig. 1*C*) and ameloblasts (*am*) but remained intense in the dental pulp (*pu*) and predentin (*pd*). To summarize, heparan sulfate in dental epithelial and mesenchymal cells is desulfated during their differentiation into ameloblasts and odontoblasts.

Expression of Sulf1 and Sulf2 in Developing Root—We evaluated the mRNA expression of *Sulf1* and *Sulf2* during tooth development. At E16.5, *Sulf1* transcripts were present in the inner enamel epithelium (*iee*), stellate reticulum (*sr*), outer enamel epithelium (*oee*), and the dental mesenchyme (*dm*) (Fig. 2*A*). At P0, *Sulf1* transcripts were detected in the stratum intermedium (*si*) as well as the stellate reticulum (*sr*) and the outer enamel epithelium (*oee*) (Fig. 2*B*). In the inner enamel epithelium (*iee*), *Sulf1* transcripts were only present in the cervical regions of the inner enamel epithelium (*iee*) (Fig. 2, *B* and *C*), and they were not detected in the differentiated ameloblasts

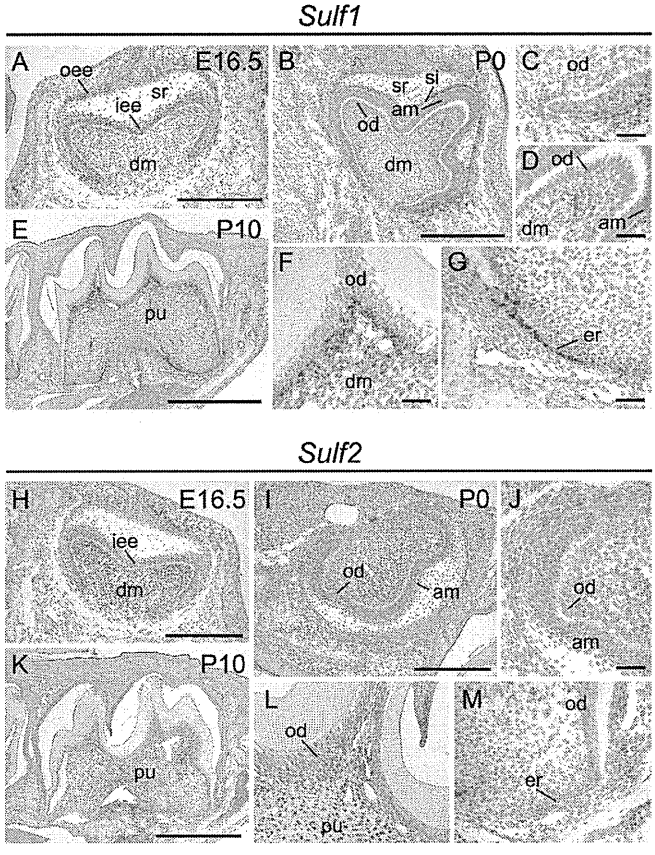

FIGURE 2. **The expression pattern of *Sulf1* (*A–G*) and *Sulf2* (*H–M*) mRNA in frontal sections of developing teeth.** *A*, at E16.5, *Sulf1* transcripts were present in the inner enamel epithelium (*iee*), stellate reticulum (*sr*), outer enamel epithelium (*oee*), and the dental mesenchyme (*dm*). *B*, at P0, *Sulf1* transcripts were detected in the stratum intermedium (*si*) as well as the stellate reticulum, the outer enamel epithelium, and the cervical regions of the inner enamel epithelium (*C*) but not in the differentiated ameloblasts (*am*) (*D*). *E*, at P10, *Sulf1* expression was present in the dental pulp (*pu*), and the signals were particularly intense in the cells underlying the differentiated odontoblasts (*F*). At the growing root apex, *Sulf1* mRNA expression was intense in the epithelial root sheath (*er*) (*G*). *H*, *Sulf2* transcripts were intensely detected throughout the dental mesenchyme at E16.5. *Sulf2* signals were also present in the inner enamel epithelium. *I*, at P0, *Sulf2* transcripts were present in the dental mesenchymal cells, including odontoblasts (*od*) (*J*). *K*, at P10, *Sulf2* expression was retained in the pulpal mesenchymal cells, except in the differentiated odontoblasts (*L*). *Sulf2* signals were detected in the differentiating odontoblasts overlying the epithelial sheath (*M*). *Scale bars*, 200 μm (*A*, *B*, *H*, and *I*), 20 μm (*C*, *D*, *F*, *G*, *J*, *L*, and *M*), and 500 μm (*E* and *K*).

(*am*) (Fig. 2, *B* and *D*). At P10, *Sulf1* expression was present in the dental pulp (*pu*) (Fig. 2*E*), and the signals were particularly intense in the cells underlying the differentiated odontoblasts (*od*) (Fig. 2*F*). In the growing root apex, *Sulf1* mRNA expression was intense in the epithelial root sheath (*er*), and signals were also detected in the differentiating odontoblasts underlying the root sheath (Fig. 2*G*).

Sulf2 transcripts were intensely detected throughout the dental mesenchyme (*dm*) at E16.5 (Fig. 2*H*). *Sulf2* signals were also present in the inner enamel epithelium (*iee*) (Fig. 2*H*). At P0, *Sulf2* transcripts were present in the dental mesenchymal cells, including odontoblasts (*od*) (Fig. 2, *I* and *J*), but its expression was significantly down-regulated in the inner enamel epithelium (*iee*) (Fig. 2*J*). At P10, *Sulf2* expression was retained in the pulpal mesenchymal cells (*pu*) (Fig. 2*K*) except in the differentiated odontoblasts (*od*) (Fig. 2*L*). *Sulf2* signals were detected in the differentiating odontoblasts overlying the epithelial sheath (*er*) (Fig. 2*M*).

Dentin Hypoplasia in Sulf Mutant Mice—We next examined the phenotypes of teeth in the control (*Sulf1*$^{+/+}$;*Sulf2*$^{+/+}$), *Sulf1* single null mutant (*Sulf1*$^{-/-}$;*Sulf2*$^{+/+}$), *Sulf2* single null mutant (*Sulf1*$^{+/+}$;*Sulf2*$^{-/-}$), and *Sulf1*/*Sulf2* double null mutant (*Sulf1*$^{-/-}$;*Sulf2*$^{-/-}$) mice. All lower molars had finished erupting in both the control and mutant littermates by P28, and the mutants did not show any tooth eruption delay. The roots of the *Sulf1*/*Sulf2* double mutant molars were short (Fig. 3*D*), but there were no differences in the size or shape of the *Sulf1* or *Sulf2* single null mice molars as compared with those of control mice (Fig. 3, *A–C*). These tooth phenotypes were further evaluated in detail by micro-CT scanning. The x-ray-opaque appearances of the enamel and dentin were not changed in the mutant teeth (Fig. 3, *E–H*). Tooth morphology was further evaluated on micro-CT-reconstructed images (Fig. 3, *I–L*). The anteroposterior length of the crown did not show any differences among the groups (Fig. 3*J*), whereas the root length was 30% shorter in the *Sulf1*/*Sulf2* mutant teeth (Fig. 3*I*). The dentin thickness in the cement-enamel junction was also reduced by 30% in the double mutant mice (Fig. 3*K*). This tooth hypoplasia phenotype displayed 100% penetration with little variation in severity. In contrast, enamel thickness was not affected (Fig. 3*L*).

Then we evaluated the neonatal phenotypes of the *Sulf1*/*Sulf2* double mutant mice in further detail. At P0, *Sulf1* and *Sulf2* deficiency resulted in a significant reduction of predentin (*pd*) thickness (Fig. 4, *A–C*). Next, we asked whether the deletion of *Sulf1* and *Sulf2* affects the sulfation state of cell surface HSPG in odontogenic cell regions. To answer this, we evaluated the changes in 10E4 and 3G10 immunoreactivity in odontoblasts and the surrounding cells. We have shown that the 10E4 immunoreactivity in the odontoblast layer decreased with differentiation (Fig. 1, *A–C*), and 10E4 staining was almost completely abolished in the odontoblast layer in the P0 control mice (*arrowheads* in Fig. 4*D*), whereas no such reduction in immunoreactivity was observed in the *Sulf1* and *Sulf2* double null mutant molars (Fig. 4*E*). These findings strongly suggested that Sulf proteins are involved in the desulfation of odontoblasts, and, as a consequence, their deficiency results in the oversulfation of these dentinogenic cells. To verify that the changed 10E4 staining in odontoblasts due to Sulf deficiency reflects a specific change in its HS sulfation status, we also examined the distribution of HS as recognized by the 3G10 antibody. 3G10 specifically identifies a neoepitope generated by heparinase III digestion of HS (50). We observed ubiquitous 3G10 staining in both the dental mesenchyme and the surrounding bones, similar to that of 10E4. There was less staining in the dental epithelium, including the stellate reticulum. Unlike 10E4 staining, which was significantly reduced in differentiated odontoblasts, 3G10 staining remained unchanged with differentiation of the odontoblast layer. In addition, the distribution of 3G10 immunoreactivity in odontoblasts and surrounding dental mesenchyme was not changed by *Sulf1*/*Sulf2* deficiency (Fig. 4, *F* and *G*). These findings indicated that the HS distribution was not affected by odontoblast differentiation or by Sulf deficiency. Thus, the increase in 10E4 immunoreactivity, as specifically

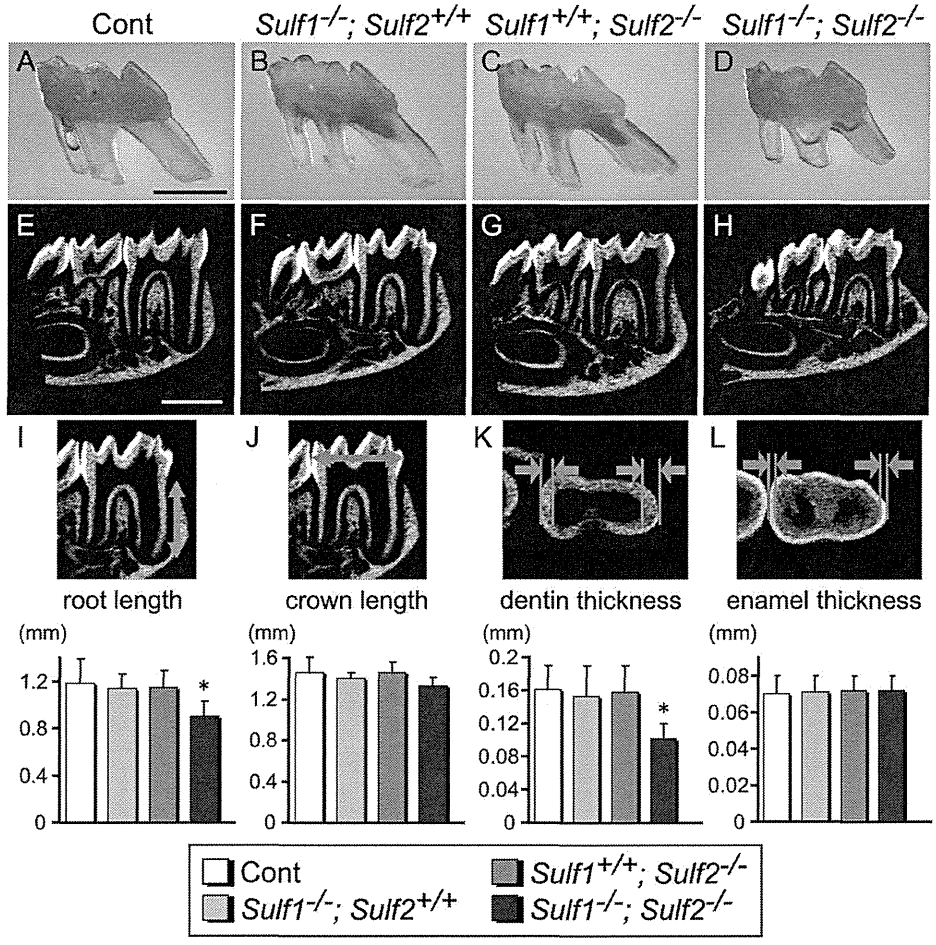

FIGURE 3. **Decreased dentin thickness and shortening of the root length in *Sulf1/Sulf2* double null mice.** *A–D*, lateral views of the first upper molars of the control (*A*, *Sulf1*$^{+/+}$;*Sulf2*$^{+/+}$), *Sulf1* single null mutant (*B*, *Sulf1*$^{-/-}$;*Sulf2*$^{+/+}$), *Sulf2* single null mutant (*C*, *Sulf1*$^{+/+}$;*Sulf2*$^{-/-}$), and *Sulf1/Sulf2* double null mutant (*D*, *Sulf1*$^{-/-}$;*Sulf2*$^{-/-}$) mice at P28. The roots of the *Sulf1/Sulf2* double null mutant molars were short. *E–H*, micro-CT-reconstructed lateral images of the first lower molars of the control (*E*), *Sulf1* single null mutant (*F*), *Sulf2* single null mutant (*G*), and *Sulf1/Sulf2* double null mutant (*H*). The *Sulf1/Sulf2* double null mutant molars showed decreased dentin thickness. *I–L*, tooth morphology was further evaluated on the micro-CT reconstructed images ($n = 12$ in control, 6 in *Sulf1*$^{-/-}$;*Sulf2*$^{+/+}$, 9 in *Sulf1*$^{+/+}$;*Sulf2*$^{-/-}$, 5 in *Sulf1*$^{-/-}$;*Sulf2*$^{-/-}$, $p < 0.001$). The root length of the mesial root (*I*) and the anteroposterior length of the crown (*J*) were measured on the reconstructed sagittal images of the lower first molars. Anteroposterior dentin (*K*) and enamel thickness (*L*) were measured on the reconstructed occlusal images. *I*, root length and dentin thickness were significantly reduced in *Sulf1/Sulf2* double null mutant molars. *Scale bars*, 1 mm (*A*) and 500 μm (*E*). *Error bars*, S.D.

observed in Sulf-deficient odontoblasts, reflects changes in the HS sulfation status of these dentinogenic cells.

Epithelial and mesenchymal proliferation in the developing tooth germs was assessed by BrdU immunohistochemistry. Many BrdU-positive cells were identified in the first molars of the mutants and control, and there was no difference in BrdU incorporation in the epithelial or mesenchymal tissue between them (Fig. 4, *H* and *I*). Then we asked why thinner dentin walls and shortened roots were produced in the *Sulf1/Sulf2* double mutant mice. Because Dspp is a tooth-specific extracellular matrix molecule and *Dspp* null mutant mice display similar tooth phenotypes as those observed in our *Sulf1/Sulf2* mutant mice (reduced dentin thickness and shortened roots), we asked whether the aberrant expression of *Dspp* mRNA contributes to the *Sulf* double null mutant dentin phenotype. In the control molars at P0, a strong *Dspp* mRNA signal was detected in odontoblasts (Fig. 4*J*), whereas a slight reduction in *Dspp* was observed in the *Sulf1/Sulf2* null mutant molars (Fig. 4*K*). In addition, total RNA was isolated from these mice, and real-time PCR also revealed a significant reduction in the *Dspp* mRNA expression in *Sulf1/Sulf2* null mutant teeth ($p < 0.005$; Fig. 4*N*). Taken together, the loss of function of *Sulf1* and *Sulf2* induced dentin hypoplasia and shortening of the root accompanied by the inhibition of desulfation in the differentiated odontoblast layer and the down-regulation of *Dspp* expression.

Desulfation Affects Dspp mRNA Expression through Wnt Signaling Pathway—To investigate the mechanisms underlying Sulf regulation of *Dspp* expression, we utilized *in situ* hybridization and biochemical and cell culture assays. Recent *TOPGAL* staining data and *Axin2* expression data suggested that the Wnt canonical pathway is activated in dentinogenesis (23, 24). This pathway is known to be promoted through Sulf activity (38). In the control molars at P0, *Axin2* mRNA signal was detected in odontoblasts and slightly in the periodontal ligaments (Fig. 4, *L* and *L'*), whereas a reduction in *Axin2* was observed in the *Sulf1/Sulf2* null mutant molars (Fig. 4, *M* and *M'*). Real-time PCR also revealed a significant reduction in

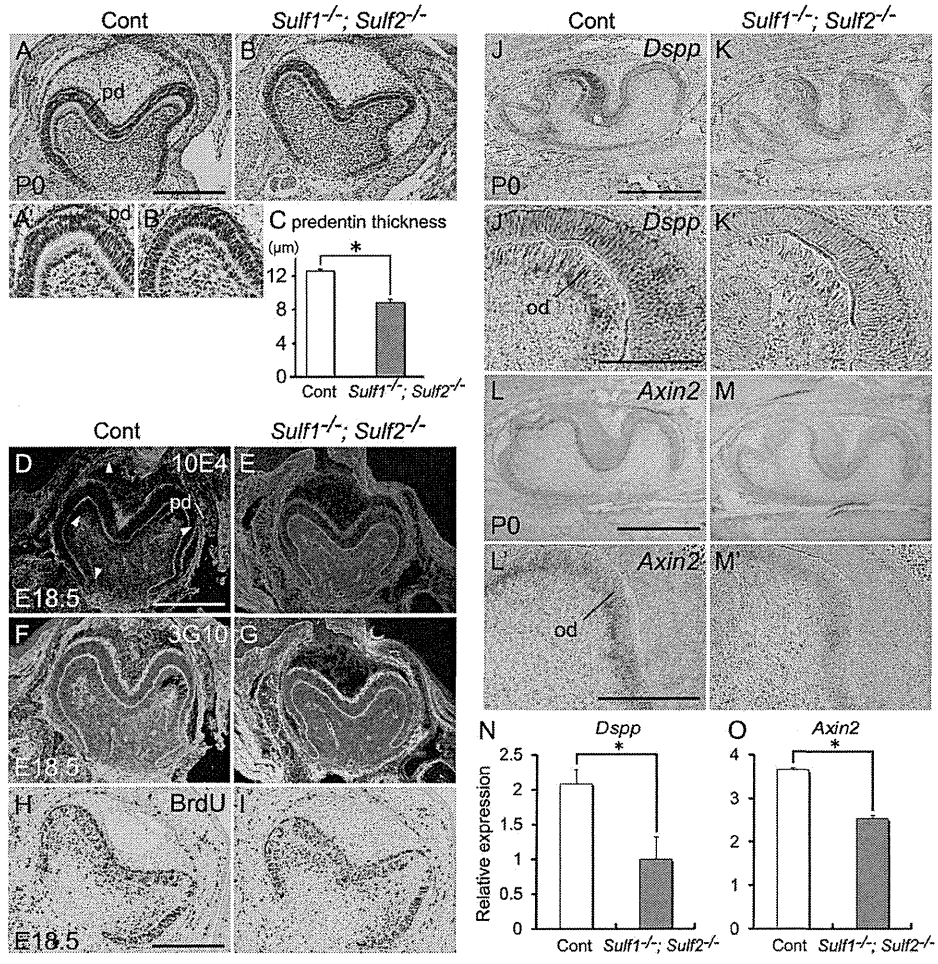

FIGURE 4. **Molar tooth phenotypes of the *Sulf1/Sulf2* mutant mice.** *A* and *B*, frontal sections of the first lower molars of the control (*A*, *Sulf1*$^{+/+}$;*Sulf2*$^{+/+}$) and *Sulf1/Sulf2* double null mutant (*B*, *Sulf1*$^{-/-}$;*Sulf2*$^{-/-}$) mice at P0. Odontoblasts were observed in both the control and mutant molars. *A'* and *B'*, higher magnification views of the predentin beneath the mesial cusps of the control (*A*) and *Sulf1/Sulf2* double null mutant (*B*) molars. Predentin (*pd*) was observed in both the control and *Sulf1/Sulf2* mutant molars and was thinner in the *Sulf1/Sulf2* mutant molars. *C*, quantification of the predentin thicknesses shown in *A* and *B*. The predentin thickness was reduced by 30% in the *Sulf1/Sulf2* double null mutant molars ($n = 4$ in each group, $p < 0.001$). *D* and *E*, immunofluorescent staining of 10E4 in the control (*D*) and *Sulf1/Sulf2* double null mutant (*E*) lower molars. The 10E4 immunoreactivity was significantly suppressed in the differentiated odontoblasts and ameloblasts in the control molars (*D*). No such suppression of 10E4 immunoreactivity was observed in the *Sulf1/Sulf2* mutant molars (*E*). *F* and *G*, immunofluorescent staining of 3G10 in the control (*F*) and *Sulf1/Sulf2* double null mutant (*G*) lower molars. 3G10 immunoreactivity was not changed by *Sulf1/Sulf2* deficiency. *H* and *I*, BrdU incorporation was not affected in the mutant molars. *J* and *K*, *Dspp* mRNA expression in the control (*J*) and *Sulf1/Sulf2* double null mutant (*K*) lower molars. *Dspp* mRNA expression was observed in both the control and mutant molars but was reduced in the mutant molars. *L* and *M*, *Axin2* mRNA expression in the control (*L*) and *Sulf1/Sulf2* double null mutant (*M*) lower molars. *Axin2* mRNA expression was observed in both control and mutant molars but was reduced in mutant molars. *J'–M'*, high magnification images of *Dspp* and *Axin2* mRNA expression in the control (*J'* and *L'*) and *Sulf1/Sulf2* double null mutant (*K'* and *M'*) molars. *N* and *O*, total RNA was isolated from the whole tooth germs of P0 control and *Sulf1/Sulf2* double null mice. There was a significant reduction in the *Dspp* (*N*) and *Axin2* (*O*) mRNA expression in *Sulf1/Sulf2* null mutant teeth ($p < 0.005$ and $p < 0.01$, respectively). *Scale bars*, 200 μm (*A*, *D*, and *H*), 500 μm (*J* and *L*), and 100 μm (*J'* and *L'*). *Error bars*, S.D.

Axin2 mRNA expression in *Sulf1/Sulf2* null mutant teeth ($p < 0.01$; Fig. 4*O*).

We then tested whether Wnt signaling modulates *Dspp* expression in the odontoblast-like mDP cell line. LiCl, an inhibitor of glycogen synthase kinase-3, was used to activate Wnt signaling (41). Mimicking Wnt signaling with 5 or 50 mM LiCl treatment for 5 days resulted in the up-regulation of *Dspp* expression in a dose-dependent manner (Fig. 5*A*), which strongly suggests that *Dspp* mRNA expression is regulated, at least in part, by the Wnt canonical signaling pathway.

We evaluated the possible changes of 10E4 immunoreactivity in mDP cells (Fig. 5*B*). All cells displayed cell surface 10E4 immunoreactivity, which was reduced upon transfecting these cells with *Sulf1* (Fig. 5*B*). In contrast, there was no difference in 3G10 immunoreactivity between transfected and control cells (Fig. 5*C*). These findings indicated that the sulfation status but not the amount and distribution of HS was affected by Sulf1.

We then attempted to confirm the physiological functions of Sulf proteins related to the tooth phenotype *in vitro* and to investigate the mechanism by which Sulf-mediated desulfation promotes Wnt signaling and the subsequent modulation of *Dspp* expression *in vitro*. Our *in vivo* findings showed that differentiating odontoblasts express both *Sulf1* and *Sulf2*; however, the mDP cells predominantly express *Sulf2* mRNA with little *Sulf1* expression. Hence, to confirm the functional roles of endosulfatases *in vitro*, we transfected cells with a plasmid encoding an miRNA to down-regulate *Sulf2* expression and GFP to enable identification of the transfected cells expressing

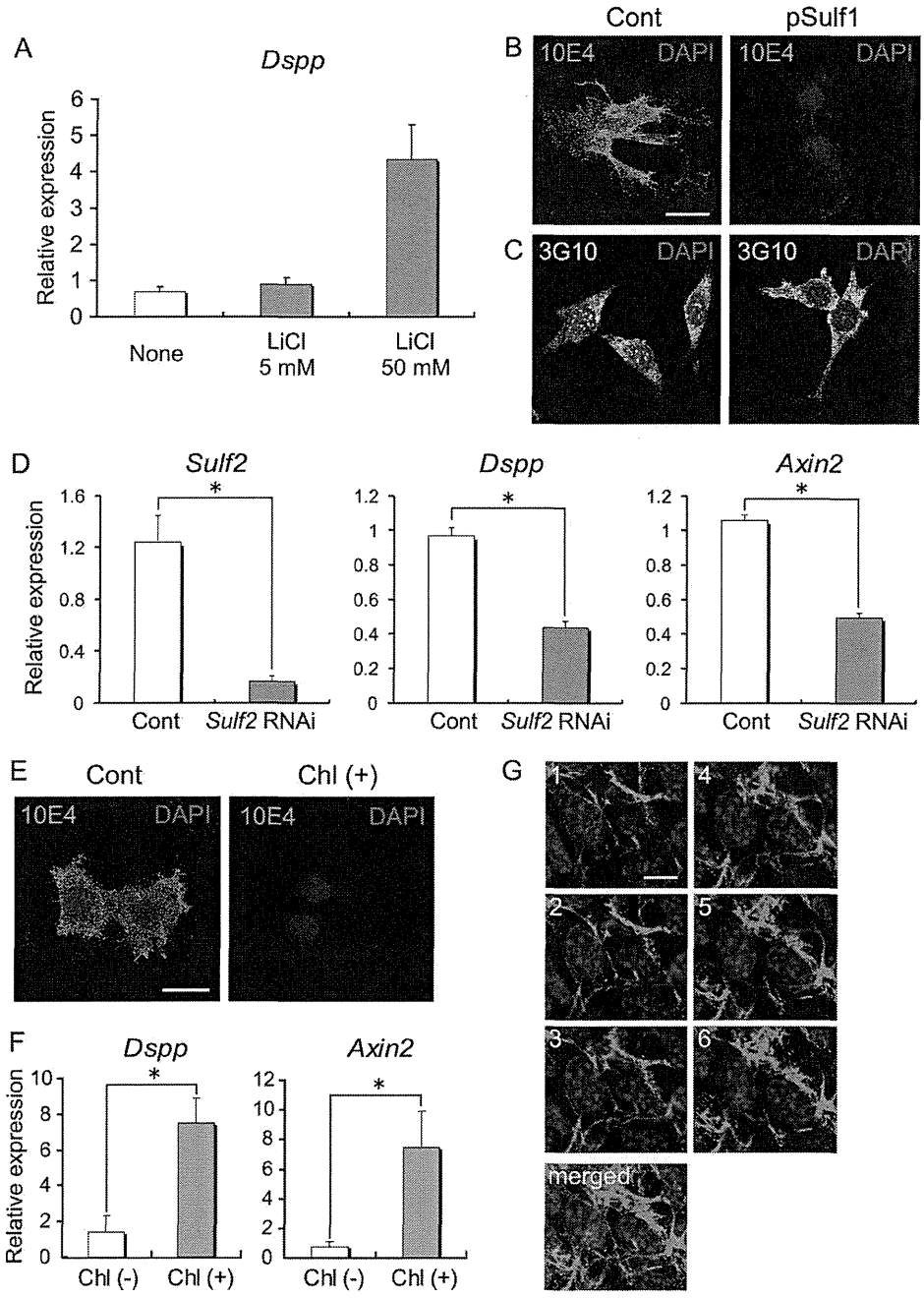

FIGURE 5. **Sulfation of cell surface HSPG affects *Dspp* mRNA expression through the modulation of the Wnt canonical signaling pathway in odontoblasts.** *A*, LiCl, an inhibitor of glycogen synthase kinase-3, was used to activate Wnt signaling. LiCl treatment for 5 days resulted in the up-regulation of *Dspp* expression in a dose-dependent manner. *B*, *Sulf1* overexpression resulted in a marked reduction in 10E4 immunoreactivity (*C*) but not in 3G10 immunoreactivity. *D*, *Sulf1* and *Sulf2* mRNA was observed in odontoblasts in our *in vivo* study; however, mDP cells predominantly expressed *Sulf2* and only slightly expressed *Sulf1*. Hence, a plasmid encoding an miRNA for down-regulating *Sulf2* expression was transfected into the cells. RNAi silencing of *Sulf2* resulted in the down-regulation of *Dspp* and *Axin2* mRNA expression in the mDP cells ($p < 0.01$). *E*, chlorate treatment resulted in a marked reduction in the binding of the 10E4 antibody to mDP cells. *F*, chlorate treatment up-regulates *Dspp* mRNA expression together with the increased expression of *Axin2* mRNA ($p < 0.05$). *G*, tomographic images of immunohistochemical localization of 10E4 immunoreactivity by confocal laser-scanning microscopy. Tomographic images are shown at 0.25-μm intervals (*1–6*) and merged into a *stacked image* (*bottom*). Each confocal image stack demonstrated that 10E4 immunoreactivity was detected on the cell surface. *Scale bars*, 20 μm (*B* and *E*) and 10 μm (*G*). *Error bars*, S.D.

the *Sulf2* miRNA. Using immunofluorescence, we verified that 120 h after the transfection, almost 95% of the mDP cells were GFP-positive. Real-time PCR demonstrated that miRNA against mouse *Sulf2* decreased the mRNA expression levels of *Sulf2* by 90% relative to the mock vector-treated control (Fig. 5*D*). Real-time PCR also demonstrated that *Sulf2* miRNA treatment attenuated *Dspp* mRNA expression together with *Axin2* expression (Fig. 5*D*).

Sodium chlorate is a competitive inhibitor of the formation of the sulfate donor required for sulfation during HS biosynthesis (40), and we confirmed that chlorate treatment resulted in a marked reduction in the binding of 10E4 antibody to mDP cells

(Fig. 5*E*). In addition, chlorate treatment up-regulated *Dspp* mRNA expression and also expression of *Axin2* mRNA (Fig. 5*F*). Taken together, the pharmacological interference with cell surface HSPG sulfation activates the Wnt canonical signaling pathway and consequently up-regulates *Dspp* mRNA expression; this could be further studied using *Wnt10a*-transfected cells.

Sulfation State of Cell Surface HS Modulates Wnt Canonical Signaling Pathway Induced by Wnt10a in Dentinogenesis—In a previous study, Ai *et al.* (38) demonstrated that QSulf1 removes 6-*O*-sulfates from HS chains to promote the formation of low affinity HS-Wnt complexes that can functionally interact with Frizzled receptors as a means of initiating Wnt signal transduction. In addition, we found that *Wnt10a* expression is found in odontoblast layers and also showed that Wnt10a directly induces *Dspp* expression in pluripotent mesenchymal cell lines. Taken together, we hypothesized that Sulf proteins function in dentinogenesis to control the affinity of the Wnt10a protein for HS in the extracellular matrix as a means of facilitating the binding of Wnt10a to its receptor and, consequently, of regulating the Wnt canonical signaling pathway.

To confirm the distribution of 10E4 immunoreactivity in mDP cells, 10E4 immunoreactivity was evaluated using a confocal laser-scanning microscope. Tomographic images, taken at 0.25-μm intervals, demonstrated that 10E4 immunoreactivity was detected on the cell surface (Fig. 5*G*).

Wnt10a is specifically expressed in odontoblasts and differentiating ameloblasts (Fig. 6*A*). We found that the overexpression of *Wnt10a* induced the expression of *Dspp* mRNA in mDP (Fig. 6*B*), as shown previously in 10T1/2 cells, which are pluripotent mesenchymal cell lines (26). The application of sodium chlorate further up-regulated *Dspp* and *Axin2* mRNA expression (Fig. 6*C*), indicating that reducing HS sulfation by chlorate treatment sensitizes Wnt10a, thereby inducing the Wnt canonical signaling pathway and promoting *Dspp* mRNA expression.

Wnt10a immunoreactivity was identified in the cytoplasm and on the cell surface of mDP cells (Fig. 6*D*). Chlorate treatment inhibits sulfation, and β-D-xyloside uncouples GAG synthesis from proteoglycan linkage and hence surface anchoring. Both treatments reduced the cell surface immunoreactivity of Wnt10a. These findings indicate that Wnt10a associates with sulfated cell surface GAGs (Fig. 6*D*).

Acting as an artificial primer of GAG chain synthesis β-D-xyloside may lead to release of HS without core proteins (42, 43). In fact, β-D-xyloside treatment significantly down-regulated *Dspp* expression in mDP cells. Likewise, exogenously added heparin significantly down-regulated *Dspp* expression in mDP cells (Fig. 6*E*). These findings suggest that released HS and also added heparin bind Wnt in the conditioned medium.

Wnt10a Interaction with HS Is Sensitive to 6-O-Desulfation in Vitro—To directly evaluate the specific effect of Sulf-mediated 6-*O*-desulfation of HS on Wnt10a binding, we employed affinity chromatography on immobilized HS that had been pretreated or not with recombinant Sulf1. In earlier experiments, we could show that this treatment specifically removed the 6-*O*-sulfate groups located in the trisulfated UA(2S)-GlcNS(6S) disaccharide units of HS (47). Recombinant Wnt10a, loaded as a total lysate of producer cells (Fig. 7*A*) on the untreated HS

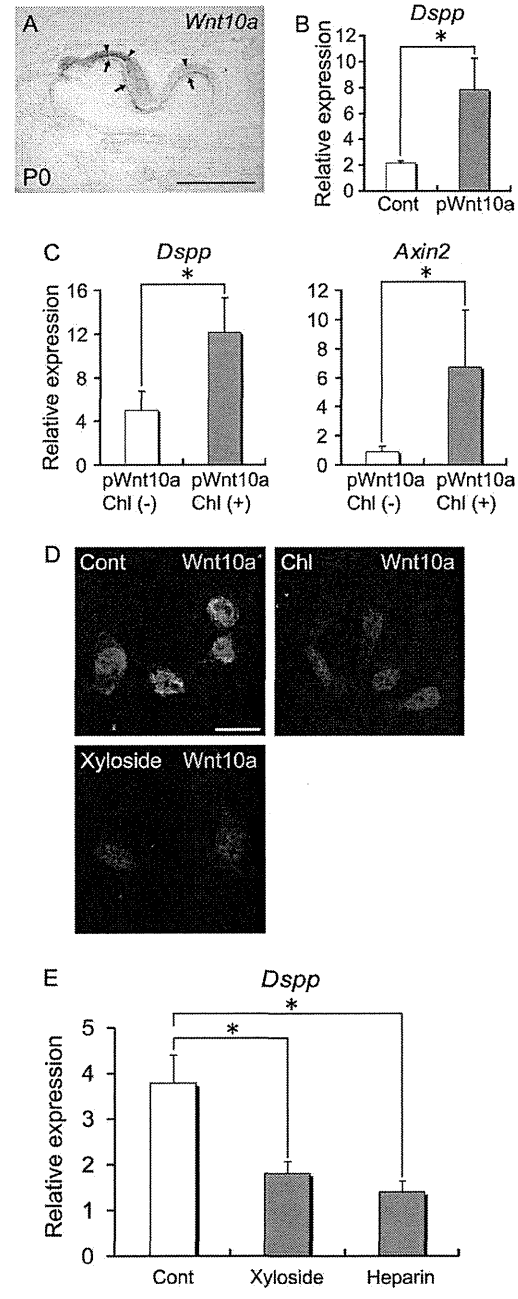

FIGURE 6. **Sulfation of cell surface HSPG modulates the Wnt canonical signaling pathway induced by Wnt10a.** *A*, at P0, *Wnt10a* mRNA was intensely detected in the odontoblast (*arrows*) and differentiating ameloblast (arrowheads) layers. *B*, the overexpression of *Wnt10a* potentiates *Dspp* mRNA expression in mDP cells, as revealed by quantitative RT-PCR ($p < 0.05$). *C*, chlorate treatment further up-regulated *Dspp* and *Axin2* mRNA expression. *D*, Wnt10a immunoreactivity was identified in the cytoplasm and the cell surfaces of mDP cells. Both chlorate treatment and β-D-xyloside treatment reduced cell surface immunoreactivity for Wnt10a. *E*, in addition, treatment with β-D-xyloside and also with heparin reduced *Dspp* mRNA expression ($p < 0.05$). *Scale bars*, 500 μm (*A*) and 20 μm (*D*). *Error bars*, S.D.

matrix, showed strong binding, as evidenced by a high salt resistance of this interaction. In a linear NaCl gradient, Wnt10a eluted from HS at a concentration of ~460 mM (Fig. 7*B*), as calculated from the conductivity measured for each eluted fraction. By contrast, Wnt10a showed a significantly reduced affinity toward Sulf1-pretreated HS, eluting at an NaCl concentra-

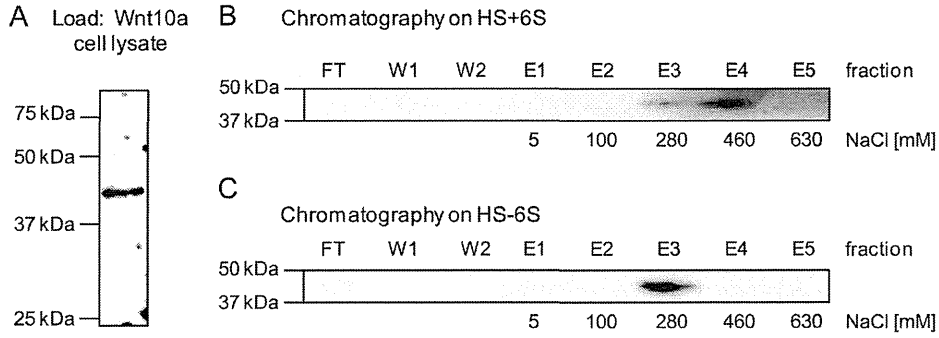

FIGURE 7. **Affinity of Wnt10a toward heparan sulfate.** *A*, Wnt10a could be specifically detected in a total lysate of producer cells by Western blotting. *B*, upon loading this lysate to immobilized heparan sulfate (*HS+6S*), all Wnt10a bound to this matrix and was eluted in a linear salt gradient at the indicated NaCl concentration given *below* each elution fraction (*FT*, flow-through; *W1* and *W2*, wash fractions; *E1–E5*, elution fractions). *C*, the salt resistance of Wnt10a binding to heparan sulfate was significantly reduced when loading the lysate on immobilized heparan sulfate that had been enzymatically 6-*O*-desulfated (*HS-6S*) by pretreatment with Sulf1. The given NaCl concentrations were calculated from conductivity measurements in each of the elution fractions.

tion of ~280 mM (Fig. 7*C*). Thus, Sulf1 directly affects Wnt10a binding to HS.

DISCUSSION

This study presents the first molecular evidence for the functional roles of HS sulfation in dentinogenesis. We found that the cell surface HSPGs of odontoblasts are desulfated during odontoblast differentiation. The endosulfatases Sulf1 and Sulf2 are secreted to selectively remove 6-*O*-sulfate groups from cell surface HSPGs, thereby modifying their affinity toward signaling molecules. We demonstrate that the loss of endosulfatases results in degenerative phenotypes elicited by disturbed dentin matrix formation. We found that the postsynthetic removal of sulfate moieties from HSPGs modifies the Wnt canonical signaling pathway in cells of the odontogenic lineage, which regulates the expression of *Dspp*, a dentin-specific matrix protein. We also found that HSPGs provide binding sites for Wnt10a and that specific desulfation regulates the binding affinity between Wnt10a and HSPGs as a means of modulating the canonical Wnt signaling pathway.

Desulfation and Odontoblast Differentiation—HSPGs are found at the cell surface and also associated with the basement membrane (51). Tooth development is regulated by epithelial-mesenchymal interactions in the basement membrane, which is located between differentiating odontoblasts and ameloblasts and provides a scaffold for their differentiation. Our 10E4 immunocytochemistry indicated that HSPGs are ubiquitously sulfated both at the cell surface and the basement membrane in developing tooth germs during early tooth development.

In odontogenesis, odontoblasts gradually lost their immunoreactivity for 10E4 during their maturation, whereas pulp cells retained their positive immunoreactivity, indicating that HSPGs are specifically desulfated during odontoblast differentiation. The 10E4 antibody has been used previously to demonstrate Sulf-mediated HS desulfation (38, 52, 53); however, it is unclear which epitope the 10E4 antibody recognizes. If 10E4 recognizes HS in general, the decreased 10E4 immunostaining levels might indicate that 6-*O*-desulfation affects the turnover of cell surface HS/HSPGs. Therefore, we also evaluated 3G10 immunoreactivity in the control and mutant tooth germs and odontoblast cell lines. 3G10 antibody identifies a neoepitope generated by heparinase III digestion of HS (50), and the 3G10 immunocytochemical study clearly showed that distribution of HS/HSPGs in odontoblasts was changed neither by its differentiation nor by *Sulf1/Sulf2* deficiency *in vivo* or by forced expression of *Sulf1 in vitro*. Therefore, decreased 10E4 immunostaining levels in the odontoblast layer obviously are due to 6-*O*-desulfation of HS/HSPGs.

Our *in vitro* study confirmed the presence of 10E4 immunoreactivity on the cell surfaces of odontoblast cell lines and showed that the forced expression of *Sulf1*, which selectively desulfates 6-*O*-sulfated residues, almost completely diminished the immunoreactivity to 10E4. Furthermore, gene ablation of *Sulf1* and *Sulf2* led to the suppression of differentiation-associated HSPG desulfation in odontoblasts. Taken together, *Sulf1* and *Sulf2* are essential for temporally and spatially regulating the 6-*O*-desulfation of odontogenic cells during their differentiation.

In contrast to the specific desulfation of odontoblast cell surface HSPGs during differentiation, 10E4 immunoreactivity on the basement membrane was not affected by odontoblast differentiation or by *Sulf1* or *Sulf2* deficiency. During progressive tooth development, the direct interaction between the epithelium and mesenchyme is degraded when these cells start to secrete the matrix on the basal membrane side, and the basement membrane is replaced with predentin. Actually, a previous study showed that immunoreactivity to perlecan, an extracellular matrix HSPG, is intense in the basement membrane and is continuously detected in areas of predentin during the production of the dentin matrix (54). As in the basement membrane, 10E4 immunoreactivity was also present in the predentin regions, but it was not affected by odontoblast differentiation or by *Sulf1* or *Sulf2* deficiency. These findings indicate that matrix HSPGs in the basement membrane are highly sulfated, whereas predentin shows little sulfation during tooth development. Therefore, it is likely that their functional roles differ from the differentiation-associated regulatory role of cell surface HSPGs.

Defective Phenotypes of Sulf1- and Sulf2-deficient Molars—*Sulf1/Sulf2* double mutant mice characteristically showed dentin and predentin thinning and shortening of their roots. Because the morphology and size of the molars and enamel thickness were not affected by *Sulf1* and *Sulf2* deficiency, tooth

phenotypes are odontogenic lineage cell specific. Significantly, Sulf proteins are not essential for odontoblast differentiation itself because odontoblast cells in *Sulf1/Sulf2* null mutant tooth also exhibit a columnar shape with predentin formation. On the other hand, the Sulf protein-defective phenotypes are similar to *Dspp* null mutant phenotypes. Human *DSPP* mutations also cause hypodontia and/or oligodontia. Our *in vitro* study also confirmed the functional roles of Sulf proteins in odontoblasts, and actually, the down-regulation of *Sulf2* by RNAi suppressed *Dspp* expression in odotoblastic cell lines. The down-regulation of *Dspp* and *Axin2* mRNA expression was also observed *in vivo* in *Sulf1/Sulf2* mutant molars by *in situ* hybridization. Real-time PCR also confirmed significant down-regulation of *Dspp* and *Axin2* mRNA expression in the mutant tooth germs. These data provide the first direct genetic evidence that the Sulf enzymes are specifically involved in dentinogenesis in odontoblasts. Importantly, we found that the Sulfs play regulatory, but not obligatory, roles in *Dspp* expression during dentinogenesis.

Because the individual knock-out of *Sulf1* or *Sulf2* did not produce altered tooth phenotypes, Sufl1 and Sulf2 display functional redundancy in dentinogenesis. This redundancy was also evident in skeletogenesis (35).

Activation of Wnt Canonical Signaling Pathway in Dentinogenesis—Dspp expression is influenced by various growth signaling molecules, such as BMP, FGF, and Wnt, in a complexed manner *in vivo*. Sulf proteins also modulate the function of heparan sulfate by altering the binding sites for these signaling molecules. It is established that Sulf proteins are negative regulators of FGF signaling and positive regulators of Wnt signaling. Our mutant phenotypes revealed that Sulf proteins are positive regulators of dentinogenesis, and previous studies have demonstrated that the Wnt canonical signaling pathway is activated in dentinogenesis. Although FGF signaling is also activated in dentinogenesis, we hypothesize that Wnt signaling is the main target of Sulf-mediated HSPG modification during dentinogenesis.

The activation of the canonical Wnt signaling pathway can be achieved with LiCl. Our attempt to mimic Wnt signaling with LiCl clearly indicated the functional importance of Wnt canonical signaling in *Dspp* mRNA induction in odontoblasts. Although the findings suggested that the Wnt canonical signaling pathway is involved in dentinogenesis, our results are the first to provide direct evidence that Wnt canonical signaling is involved in the promotion of *Dspp* mRNA expression.

In our study, chlorate treatment, which pharmacologically blocked sulfation of cell surface HSPGs (40), up-regulated *Dspp* mRNA expression in odontoblasts and induced *Axin2* mRNA expression. On the contrary, the *Sulf2* RNAi-induced down-regulation of *Dspp* expression was accompanied by the suppression of *Axin2* expression. In other developmental systems, it has been established that Sulf enzymes function as positive regulators of Wnt signaling (29, 38). Our results indicating that Sulf proteins promote Wnt signaling during dentinogenesis are in line with those previous studies.

Sulf Modification of Wnt10a-induced Signaling in Dentinogenesis—In the present study, pharmacological interference of HSPG sulfation by chlorate treatment augmented canonical Wnt signaling in mDP cells and subsequently up-regulated

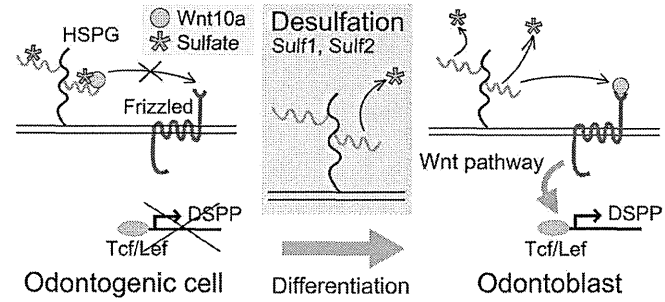

FIGURE 8. **A model of Wnt signaling regulation induced by cell surface HSPG desulfation during dentinogenesis.** Desulfation by Sulf reduces the affinity of cell surface HS for Wnt10a as a means of facilitating Wnt10a binding to its receptor and hence potentiating the Wnt canonical signaling pathway, which consequently up-regulates *Dspp* expression in odontoblasts.

Dspp expression in these cells. We also detected Wnt10a immunoreactivity on the cell surfaces of odontoblastic cell lines, and chlorate treatment decreased this immunoreactivity. Similarly, Wnt10a protein disappeared from the odontoblast cell surface upon a 72-h treatment with xyloside. β-D-Xyloses linked to hydrophobic aglycones act as artificial primers of GAG chain synthesis and block proteoglycan assembly (42, 43). Therefore, HS would be released without core proteins and could form a complex with Wnts, including Wnt10a, in the conditioned medium. Like β-D-xyloside treatment, exogenously added heparin also significantly down-regulated *Dspp* expression in mDP cells in the present study, suggesting that released HS, like heparin, provides binding sites for Wnt10a. Finally, our affinity chromatography data provide clear biochemical evidence for a direct physical interaction between Wnt10a and HS and demonstrate that the binding affinity of HS toward Wnt10a is reduced by 6-*O*-desulfation; it should be noted that the 6-*O*-desulfated HS used here had been generated through pretreatment of HS with recombinant Sulf1 *in vitro*, and its specific desulfation had structurally and functionally been characterized earlier (47). Taken together, these findings indicate that HSPGs on the cell surface provide binding sites for Wnt10a in odontoblasts and that specific sulfation patterns are edited post-synthetically by the Sulf enzymes, thereby regulating the binding affinity between Wnt10a and HSPGs as a means to modulate the canonical Wnt signaling pathway in dentinogenesis.

A previous study showed that Sulf proteins function autonomously to remodel the sulfation state of cell surface HS chains and promote Wnt signaling. However, there are some discrepancies among developmentally dynamic *Sulf* mRNA expression, 10E4 immunoreactivity, and *TOPGAL* reporter expression (23). Indeed, *Wnt10a* mRNA expression and *TOPGAL* reporter expression are only localized in the odontoblast layer. In contrast, *Sulf1* and *Sulf2* are only slightly expressed in odontoblasts but are intensely expressed in the dental pulpal cells overlying odontoblasts. Interestingly, desulfated regions, which are identified by their negative immunoreactivity to 10E4, were expanded in the odontoblast layer as well as the *Sulf1*- and *Sul2*-expressing layer. Hence, it is likely that the Sulfs, which are secretory proteins, also possess non-cell-autonomous or paracrine activity (36) and that odontoblasts are exposed to Sulf

proteins, which are released from the overlying pulpal cells, in a paracrine manner.

In conclusion, we found that the 6-*O*-desulfation of extracellular HSPGs is an important postsynthetic modification that is critical for the activation of Wnt signaling in odontoblasts and subsequent dentin matrix production. Notably, the loss of the Sulf 6-*O*-endosulfatases results in degenerative phenotypes elicited by disturbed dentin matrix formation. Our findings indicate that the Sulf enzymes catalyze HS 6-*O* desulfation at the cell surface of odontoblast cells and that such postsynthetic modification of the HSPG sulfation status induces Wnt10a-mediated activation of odontoblast differentiation (Fig. 8).

REFERENCES

1. Bernfield, M., Götte, M., Park, P. W., Reizes, O., Fitzgerald, M. L., Lincecum, J., and Zako, M. (1999) Functions of cell surface heparan sulfate proteoglycans. *Annu. Rev. Biochem.* **68,** 729–777
2. Plotnikov, A. N., Schlessinger, J., Hubbard, S. R., and Mohammadi, M. (1999) Structural basis for FGF receptor dimerization and activation. *Cell* **98,** 641–650
3. Reichsman, F., Smith, L., and Cumberledge, S. (1996) Glycosaminoglycans can modulate extracellular localization of the wingless protein and promote signal transduction. *J. Cell Biol.* **135,** 819–827
4. Turnbull, J., Powell, A., and Guimond, S. (2001) Heparan sulfate. Decoding a dynamic multifunctional cell regulator. *Trends Cell Biol.* **11,** 75–82
5. Ori, A., Wilkinson, M. C., and Fernig, D. G. (2008) The heparanome and regulation of cell function. Structures, functions, and challenges. *Front. Biosci.* **13,** 4309–4338
6. Tumova, S., Woods, A., and Couchman, J. R. (2000) Heparan sulfate proteoglycans on the cell surface. Versatile coordinators of cellular functions. *Int. J. Biochem. Cell Biol.* **32,** 269–288
7. Habuchi, H., Habuchi, O., and Kimata, K. (2004) Sulfation pattern in glycosaminoglycan. Does it have a code? *Glycoconj. J.* **21,** 47–52
8. Thesleff, I., Vainio, S., and Jalkanen, M. (1989) Cell-matrix interactions in tooth development. *Int. J. Dev. Biol.* **33,** 91–97
9. Thesleff, I., Partanen, A. M., and Vainio, S. (1991) Epithelial-mesenchymal interactions in tooth morphogenesis: the roles of extracellular matrix, growth factors, and cell surface receptors. *J. Craniofac. Genet. Dev. Biol.* **11,** 229–237
10. Thesleff, I., and Aberg, T. (1999) Molecular regulation of tooth development. *Bone* **25,** 123–125
11. Linde, A., and Goldberg, M. (1993) Dentinogenesis. *Crit. Rev. Oral Biol. Med.* **4,** 679–728
12. Feng, J. Q., Luan, X., Wallace, J., Jing, D., Ohshima, T., Kulkarni, A. B., D'Souza, R. N., Kozak, C. A., and MacDougall, M. (1998) Genomic organization, chromosomal mapping, and promoter analysis of the mouse dentin sialophosphoprotein (*Dspp*) gene, which codes for both dentin sialoprotein and dentin phosphoprotein. *J. Biol. Chem.* **273,** 9457–9464
13. D'Souza, R. N., Cavender, A., Sunavala, G., Alvarez, J., Ohshima, T., Kulkarni, A. B., and MacDougall, M. (1997) *J. Bone Miner. Res.* **12,** 2040–2049
14. Qin, C., Brunn, J. C., Cadena, E., Ridall, A., Tsujigiwa, H., Nagatsuka, H., Nagai, N., and Butler, W. T. (2002) The expression of dentin sialophosphoprotein gene in bone. *J. Dent Res.* **81,** 392–394
15. Shields, E. D., Bixler, D., and el-Kafrawy, A. M. (1973) A proposed classification for heritable human dentine defects with a description of a new entity. *Arch. Oral Biol.* **18,** 543–553
16. Xiao, S., Yu, C., Chou, X., Yuan, W., Wang, Y., Bu, L., Fu, G., Qian, M., Yang, J., Shi, Y., Hu, L., Han, B., Wang, Z., Huang, W., Liu, J., Chen, Z., Zhao, G., and Kong, X. (2001) Dentinogenesis imperfecta 1 with or without progressive hearing loss is associated with distinct mutations in *DSPP*. *Nat. Genet.* **27,** 201–204
17. Zhang, X., Zhao, J., Li, C., Gao, S., Qiu, C., Liu, P., Wu, G., Qiang, B., Lo, W. H., and Shen, Y. (2001) *DSPP* mutation in dentinogenesis imperfecta Shields type II. *Nat. Genet.* **27,** 151–152
18. Rajpar, M. H., Koch, M. J., Davies, R. M., Mellody, K. T., Kielty, C. M., and Dixon, M. J. (2002) Mutation of the signal peptide region of the bicistronic gene *DSPP* affects translocation to the endoplasmic reticulum and results in defective dentine biomineralization. *Hum. Mol. Genet.* **11,** 2559–2565
19. Sreenath, T., Thyagarajan, T., Hall, B., Longenecker, G., D'Souza, R., Hong, S., Wright, J. T., MacDougall, M., Sauk, J., and Kulkarni, A. B. (2003) Dentin sialophosphoprotein knockout mouse teeth display widened predentin zone and develop defective dentin mineralization similar to human dentinogenesis imperfecta type III. *J. Biol. Chem.* **278,** 24874–24880
20. Nusse, R. (2003) Wnts and Hedgehogs. Lipid-modified proteins and similarities in signaling mechanisms at the cell surface. *Development* **130,** 5297–5305
21. Cardigan, R. A., Mackie, I. J., and Machin, S. J. (1997) Hemostatic-endothelial interactions. A potential anticoagulant role of the endothelium in the pulmonary circulation during cardiac surgery. *J. Cardiothorac. Vasc. Anesth.* **11,** 329–336
22. Sarkar, L., and Sharpe, P. T. (1999) Expression of Wnt signaling pathway genes during tooth development. *Mech. Dev.* **85,** 197–200
23. Suomalainen, M., and Thesleff, I. (2010) Patterns of Wnt pathway activity in the mouse incisor indicate absence of Wnt/β-catenin signaling in the epithelial stem cells. *Dev. Dyn.* **239,** 364–372
24. Lohi, M., Tucker, A. S., and Sharpe, P. T. (2010) Expression of Axin2 indicates a role for canonical Wnt signaling in development of the crown and root during pre- and postnatal tooth development. *Dev. Dyn.* **239,** 160–167
25. Lammi, L., Arte, S., Somer, M., Jarvinen, H., Lahermo, P., Thesleff, I., Pirinen, S., and Nieminen, P. (2004) Mutations in AXIN2 cause familial tooth agenesis and predispose to colorectal cancer. *Am. J. Hum. Genet.* **74,** 1043–1050
26. Yamashiro, T., Zheng, L., Shitaku, Y., Saito, M., Tsubakimoto, T., Takada, K., Takano-Yamamoto, T., and Thesleff, I. (2007) Wnt10a regulates dentin sialophosphoprotein mRNA expression and possibly links odontoblast differentiation and tooth morphogenesis. *Differentiation* **75,** 452–462
27. Adaimy, L., Chouery, E., Megarbane, H., Mroueh, S., Delague, V., Nicolas, E., Belguith, H., de Mazancourt, P., and Megarbane, A. (2007) Mutation in WNT10A is associated with an autosomal recessive ectodermal dysplasia. The odonto-onycho-dermal dysplasia. *Am. J. Hum. Genet.* **81,** 821–828
28. Nawaz, S., Klar, J., Wajid, M., Aslam, M., Tariq, M., Schuster, J., Baig, S. M., and Dahl, N. (2009) WNT10A missense mutation associated with a complete odonto-onycho-dermal dysplasia syndrome. *Eur. J. Hum. Genet.* **17,** 1600–1605
29. Dhoot, G. K., Gustafsson, M. K., Ai, X., Sun, W., Standiford, D. M., and Emerson, C. P., Jr. (2001) Regulation of Wnt signaling and embryo patterning by an extracellular sulfatase. *Science* **293,** 1663–1666
30. Morimoto-Tomita, M., Uchimura, K., Werb, Z., Hemmerich, S., and Rosen, S. D. (2002) Cloning and characterization of two extracellular heparin-degrading endosulfatases in mice and humans. *J. Biol. Chem.* **277,** 49175–49185
31. Kalus, I., Salmen, B., Viebahn, C., von Figura, K., Schmitz, D., D'Hooge, R., and Dierks, T. (2009) Differential involvement of the extracellular 6-*O*-endosulfatases Sulf1 and Sulf2 in brain development and neuronal and behavioral plasticity. *J. Cell Mol. Med.* **13,** 4505–4521
32. Lamanna, W. C., Kalus, I., Padva, M., Baldwin, R. J., Merry, C. L., and Dierks, T. (2007) The heparanome. The enigma of encoding and decoding heparan sulfate sulfation. *J. Biotechnol.* **129,** 290–307
33. Ai, X., Kitazawa, T., Do, A. T., Kusche-Gullberg, M., Labosky, P. A., and Emerson, C. P., Jr. (2007) SULF1 and SULF2 regulate heparan sulfate-mediated GDNF signaling for esophageal innervation. *Development* **134,** 3327–3338
34. Langsdorf, A., Do, A. T., Kusche-Gullberg, M., Emerson, C. P., Jr., and Ai, X. (2007) Sulfs are regulators of growth factor signaling for satellite cell differentiation and muscle regeneration. *Dev. Biol.* **311,** 464–477
35. Ratzka, A., Kalus, I., Moser, M., Dierks, T., Mundlos, S., and Vortkamp, A. (2008) Redundant function of the heparan sulfate 6-*O*-endosulfatases Sulf1 and Sulf2 during skeletal development. *Dev. Dyn.* **237,** 339–353
36. Holst, C. R., Bou-Reslan, H., Gore, B. B., Wong, K., Grant, D., Chalasani, S., Carano, R. A., Frantz, G. D., Tessier-Lavigne, M., Bolon, B., French, D. M., and Ashkenazi, A. (2007) Secreted sulfatases Sulf1 and Sulf2 have overlapping yet essential roles in mouse neonatal survival. *PLoS One* **2,** e575

37. Lamanna, W. C., Baldwin, R. J., Padva, M., Kalus, I., Ten Dam, G., van Kuppevelt, T. H., Gallagher, J. T., von Figura, K., Dierks, T., and Merry, C. L. (2006) Heparan sulfate 6-*O*-endosulfatases. Discrete *in vivo* activities and functional cooperativity. *Biochem. J.* **400,** 63–73
38. Ai, X., Do, A. T., Lozynska, O., Kusche-Gullberg, M., Lindahl, U., and Emerson, C. P., Jr. (2003) QSulf1 remodels the 6-*O*-sulfation states of cell surface heparan sulfate proteoglycans to promote Wnt signaling. *J. Cell Biol.* **162,** 341–351
39. Wu, N., Iwamoto, T., Sugawara, Y., Futaki, M., Yoshizaki, K., Yamamoto, S., Yamada, A., Nakamura, T., Nonaka, K., and Fukumoto, S. (2010) PDGFs regulate tooth germ proliferation and ameloblast differentiation. *Arch. Oral Biol.* **55,** 426–434
40. Yip, G. W., Ferretti, P., and Copp, A. J. (2002) Heparan sulfate proteoglycans and spinal neurulation in the mouse embryo. *Development* **129,** 2109–2119
41. Klein, P. S., and Melton, D. A. (1996) A molecular mechanism for the effect of lithium on development. *Proc. Natl. Acad. Sci. U.S.A.* **93,** 8455–8459
42. Lugemwa, F. N., Sarkar, A. K., and Esko, J. D. (1996) Unusual β-D-xylosides that prime glycosaminoglycans in animal cells. *J. Biol. Chem.* **271,** 19159–19165
43. Fritz, T. A., and Esko, J. D. (2001) Xyloside priming of glycosaminoglycan biosynthesis and inhibition of proteoglycan assembly. *Methods Mol. Biol.* **171,** 317–323
44. Yamashiro, T., Fukunaga, T., Kobashi, N., Kamioka, H., Nakanishi, T., Takigawa, M., and Takano-Yamamoto, T. (2001) Mechanical stimulation induces CTGF expression in rat osteocytes. *J. Dent. Res.* **80,** 461–465
45. Yanagita, T., Kubota, S., Kawaki, H., Kawata, K., Kondo, S., Takano-Yamamoto, T., Tanaka, S., and Takigawa, M. (2007) Expression and physiological role of CCN4/Wnt-induced secreted protein 1 mRNA splicing variants in chondrocytes. *FEBS J.* **274,** 1655–1665
46. Lamanna, W. C., Frese, M. A., Balleininger, M., and Dierks, T. (2008) Sulf loss influences *N*-, 2-*O*-, and 6-*O*-sulfation of multiple heparan sulfate proteoglycans and modulates fibroblast growth factor signaling. *J. Biol. Chem.* **283,** 27724–27735
47. Frese, M. A., Milz, F., Dick, M., Lamanna, W. C., and Dierks, T. (2009) Characterization of the human sulfatase Sulf1 and its high affinity heparin/heparan sulfate interaction domain. *J. Biol. Chem.* **284,** 28033–28044
48. Leteux, C., Chai, W., Nagai, K., Herbert, C. G., Lawson, A. M., and Feizi, T. (2001) 10E4 antigen of Scrapie lesions contains an unusual nonsulfated heparan motif. *J. Biol. Chem.* **276,** 12539–12545
49. van den Born, J., Salmivirta, K., Henttinen, T., Ostman, N., Ishimaru, T., Miyaura, S., Yoshida, K., and Salmivirta, M. (2005) Novel heparan sulfate structures revealed by monoclonal antibodies. *J. Biol. Chem.* **280,** 20516–20523
50. David, G., Bai, X. M., Van der Schueren, B., Cassiman, J. J., and Van den Berghe, H. (1992) Developmental changes in heparan sulfate expression: in situ detection with mAbs. *J. Cell Biol.* **119,** 961–975
51. Jalkanen, M., Nguyen, H., Rapraeger, A., Kurn, N., and Bernfield, M. (1985) Heparan sulfate proteoglycans from mouse mammary epithelial cells. Localization on the cell surface with a monoclonal antibody. *J. Cell Biol.* **101,** 976–984
52. Lai, J., Chien, J., Staub, J., Avula, R., Greene, E. L., Matthews, T. A., Smith, D. I., Kaufmann, S. H., Roberts, L. R., and Shridhar, V. (2003) Loss of HSulf-1 up-regulates heparin-binding growth factor signaling in cancer. *J. Biol. Chem.* **278,** 23107–23117
53. Li, J., Kleeff, J., Abiatari, I., Kayed, H., Giese, N. A., Felix, K., *Giese, T.,* Büchler, M. W., and Friess, H. (2005) Enhanced levels of Hsulf-1 interfere with heparin-binding growth factor signaling in pancreatic cancer. *Mol. Cancer* **4,** 14
54. Ida-Yonemochi, H., Satokata, I., Ohshima, H., Sato, T., Yokoyama, M., Yamada, Y., and Saku, T. (2011) Morphogenetic roles of perlecan in the tooth enamel organ: an analysis of overexpression using transgenic mice. *Matrix Biol.* **30,** 379–388

Received: Nov. 8, 2011
Accepted: Jan. 24, 2012
Published online: Feb. 29, 2012

Review Article

Dental Regenerative Therapy using Oral Tissues

Narisato Kanamura [1], Takeshi Amemiya [1], Toshiro Yamamoto [1], Kenji Mishima [2], Masahiro Saito [3,4], Takashi Tsuji [3,4,5], Takahiro Nakamura [6,7]

1) Dental Medicine, Graduate School of Medical Science, Kyoto Prefectural University of Medicine
2) Department of Pathology, Tsurumi University School of Dental Medicine (Current affiliation: Department of Oral Pathology, Showa University Dental School)
3) Research Institute for Science and Technology, Tokyo University of Science
4) Department of Biological Science and Technology, Graduate School of Industrial Science and Technology, Tokyo University of Science
5) Organ Technologies Inc.
6) Research Center for Inflammation and Regenerative Medicine, Faculty of Life and Medical Sciences, Doshisha University
7) Department of Ophthalmology, Kyoto Prefectural University of Medicine

Abstract

Anti-Aging Medicine is a theoretical and practical science which aims to ensure the achievement of a long and healthy life. Dental medicine plays an important role in its practice. Given the substantial influence of dental/oral diseases on general health, the maintenance and improvement of oral function promotes not only dental/oral Anti-Aging but also systemic Anti-Aging as well.

The current target of Anti-Aging dental medicine is the prevention or slowing down of the age-related decline in oral function by evaluating indicators of oral function, such as dental age, periodontal age, occlusion age, swallowing age, and salivary age. In this symposium, Dr. Kenji Mishima (Department of Dentistry, Tsurumi University), speaking on "Application of Cell Transplantation Therapy to Salivary Gland Dysfunction", Dr. Masahiro Saito (Research Institute for Science and Technology, Tokyo University of Science), speaking on "Role of Tooth Regeneration in Anti-Aging Medicine" and myself, Dr. Narisato Kanemura (Dental Medicine, Graduate School of Medical Science, Kyoto Prefectural University of Medicine), speaking on "Development of a New Periodontal Tissue Regeneration Method Aimed at Anti-Aging Use", delivered presentations about the current status and future prospects of regenerative dentistry, which aims not only to prevent a decrease in oral function but also to restore it when function is lost, and introduced the latest in regenerative dentistry involving the salivary glands, teeth, oral mucosal epithelia, and periodontal ligaments. In addition, to describe collaboration between dental medicine and ophthalmology, Dr. Takahiro Nakamura (Faculty of Life and Medical Sciences, Doshisha University), speaking on "Current Status and Future Prospects of Corneal Regenerative Therapy using Oral Tissue", introduced the current status and future prospects of corneal regenerative therapy using periodontal mucosal epithelium. Summaries of these lectures are presented here. In the "Dental Regenerative Therapy using Oral Tissues" symposium at the 2011 11th Scientific Meeting of the Japanese Society of Anti-Aging Medicine, the experts were invited to report recent findings on maintenance.

KEY WORDS: oral tissue, regenerative therapy, saliva, tooth regenerative therapy, periodontal ligament

1. Application of Cell Transplantation Therapy to Salivary Gland Dysfunction

The causes of salivary gland dysfunction include refractory diseases such as Sjogren's syndrome and Stevens-Johnson syndrome, radiation therapy against head and neck cancer, and a variety of drugs [1]. Current treatments include the use of artificial saliva and oral therapy with muscarinic acetylcholine receptor agonists, which stimulate salivary secretion from residual acinar cells. Severe cases may be resistant to these treatments, and patients may develop oral cavity lesions such as mucositis, caries, or periodontal disease. In addition, as salivary gland dysfunction is a pathogenic factor in aspiration pneumonia in the elderly, serious concerns have been expressed about infection treatment methods. The possibilities of regenerative medicine have therefore been investigated, specifically the reconstruction of lost gland tissues using transplantation of exogenous salivary gland stem cells. However, cell surface markers specific to salivary gland stem cells are difficult to isolate and thus remain unknown. We have therefore focused on a cell population called "side population (SP)" cells, which can be isolated without using a cell surface marker. Since their first isolation from bone marrow as a fraction containing a high frequency of stem cells, SP cells have been analyzed in a variety of organs [2-6]. In the present study, we investigated the effects of experimental treatment with SP cells using a mouse model of irradiation-induced salivary gland dysfunction, and the possibility of establishing a treatment approach with a specific factor expressed in SP cells.

Narisato Kanamura
Dental Medicine, Graduate School of Medical Science, Kyoto Prefectural University of Medicine
Kajii-cho 465, Kawaramachi-Hirokoji, Kamigyo-ku, Kyoto 602-8566, Japan
Tel & Fax: +81-75-251-5641 / E-mail: kanamura@koto.kpu-m.ac.jp

Investigation of effects of treatment with SP cells

Salivary gland tissue collected from green fluorescent protein (GFP) transgenic mice was digested with collagenase and hyaluronidase to remove interstitial tissue, and epithelial clusters were isolated using a filter mesh. The isolated epithelial clusters were then treated with trypsin to disperse the cells, stained with Hoechst 33342, and subjected to FACS with UV laser irradiation and measurement at two wavelengths (450 nm and 675 nm). As a result, SP cells were detected as a characteristic cell population with low fluorescence intensity which accounted for about 0.5% to 1.0% of salivary gland cells. Next, Hoechst 33342-negative SP cells and Hoechst 33342-positive non-SP (main population, MP) cells were collected using FACS [7]. The collected cells were then transplanted into salivary glands of mice with irradiation-induced salivary gland dysfunction (15 Gy local irradiation). Saliva production associated with treatment with pilocarpine, a muscarinic acetylcholine receptor agonist, was then measured serially to determine the effects of SP cell transplantation. The results showed the restoration of secretion volume at 1 month after transplantation. In addition, examination of the removed tissues by fluorescence microscopy indicated the sparse distribution of GFP-positive cells. However, because the observed number of GFP-positive cells was low, the transplanted SP cells were unlikely to have directly contributed to the restoration of secretory ability, suggesting that soluble factor(s) secreted from SP cells may be involved in the secretory mechanism of residual acinar cells.

Functional analysis of SP cell-specific expression gene

Hoechst 33342-negative SP cells and Hoechst 33342-positive non-SP (main population, MP) cells were collected using FACS, and RNAs were extracted from the collected SP and MP cells using a PicoPureRNA isolation kit (Arcturus). In addition, RNA amplification was performed by a T7 polymerase-based method using a RiboAmp RNA amplification kit (Arcturus). The amplified RNAs derived from SP and MP cells were then used to synthesize cDNAs, which were fluorescence-labeled with Cy3 or Cy5 and subjected to competitive hybridization on NIA 15K mouse cDNA array (Version 2) to compare their gene expression profiles based on the detected signals. This method identified multiple genes specifically expressed in SP cells, among which we selected clusterin for functional analysis. Specifically, clusterin gene was introduced into STO cells, a mouse embryonic fibroblast cell line, by lipofection to prepare a cell line that stably expresses clusterin following drug selection. We next investigated the possible function of clusterin in reducing damage caused by reactive oxygen species (ROS), on the basis that irradiation-induced cell damage is mediated by ROS. Specifically, we counted viable cells stained using trypan blue 24 hours after stimulation of clusterin-expressing and control cells with different concentrations of hydrogen peroxide solution. The results showed significantly higher cell viability among clusterin-expressing cells than control cells, and a decrease in ROS production in the cells.

We then investigated the effects of treatment with SP cells collected from clusterin gene knockout mice to verify the involvement of clusterin in the treatment effects of SP cells. Although autoimmune myocarditis has been reported in clusterin knockout mice, we saw no histological change in 12-week-old mice at least, and no difference in SP cell fraction compared to control mice [8]. However, pilocarpine-stimulated salivation was not restored in mice with irradiation-induced salivary gland dysfunction even after transplantation of SP cells of the above-mentioned knockout mice. These findings indicated that clusterin makes a critical contribution to treatment effects in SP cell transplantation.

Verification of treatment effects of clusterin using a mouse model with salivary gland dysfunction

To determine whether clusterin directly contributes to the reversal of cellular dysfunction of the salivary gland, clusterin-expressing recombinant lentivirus (Lenti-Clu, 5 x 10^6 TU) was injected into one submandibular gland of mice with irradiation-induced salivary gland dysfunction 4 days after irradiation, and GFP-expressing lentivirus (Lenti-GFP, 5 x 10^6 TU) was injected into the other [9]. Gene transfection efficiency and time-dependent change in saliva volume were then measured to assess restoration of secretory ability. The results indicated that Lenti-GFP transfection led to GFP positivity in approximately 16% of cells. In contrast, Lenti-Clu-injected mice showed an improvement in pilocarpine-stimulated salivation at 4, 8, and 16 weeks after virus injection compared to Lenti-GFP-injected mice. These results suggested that clusterin, which is expressed in SP cells, is involved in the functional restoration of glandular secretion.

These results revealed that SP cells or clusterin, a specific factor expressed in SP cells, is effective in the treatment of irradiation-induced salivary gland dysfunction. We are planning to examine the possible clinical application of these factors in the future.

2. Role of Tooth Regeneration in Anti-Aging Medicine

Introduction

Teeth possess not only a masticatory function (*i.e.*, "chewing") but also act as sensory receptors, sending masticatory stimulation to centers in the brain. Caries and tooth loss secondary to periodontal disease, the incidence of which are increasing in the elderly, are known to cause significant problems with masticatory function and to affect systemic condition. Thus, the development of dental regenerative medicine that can essentially restore the physiology of natural teeth will be useful in preventing a decline in oral function and in promoting Anti-Aging. Here, we discuss the current status of R&D in dental regenerative therapy against tooth loss, as well as its potential role in Anti-Aging Medicine.

Tooth regeneration by a bioengineered organ germ method

Previously, functional complementary therapies with artificial devices such as dentures, dental bridges, and dental implants have been used as dental support for tooth loss. Although these complementary therapies are effective in the restoration of masticatory function, they cannot restore the innate physiological aspects of teeth, such as tooth movement associated with aging and response to masticatory stimulation.

Thus, a more biological treatment approach to tooth regeneration has been sought.

Teeth develop through continuous interaction between odontogenic epithelial cells and odontogenic mesenchymal cells which together constitute the embryonic tooth germ [10]. For this reason, technologies that enable the regeneration of tooth germ from epithelial and mesenchymal cells through three-dimensional cell manipulation techniques have been developed with the goal of regenerating third teeth, in addition to primary and permanent teeth. To date, however, the ability to produce highly effective and normal tooth development has not been reached [11]. In 2007, we developed the "bioengineered organ germ method," in which epithelial and mesenchymal cells derived from the tooth germ are compartmentally arranged at high cellular density (***Fig. 1***, top) [12]. When ectopically transplanted *in vivo*, the bioengineered tooth bud cells develop with structurally normal regenerated teeth as well as periodontal tissue (periodontal ligament, cementum, alveolar bone), indicating the potential use of bioengineered tooth bud cells in tooth regenerative therapy [12].

Regeneration of functional teeth

Successful tooth regenerative therapy requires not only the histological normality of the regenerated tooth but also its eruption/occlusion within the recipient's intraoral environment, and the full spectrum of normal tooth physiology, such as functional regeneration of the periodontal ligament and response to external noxious stimuli. When bioengineered tooth bud cells were transplanted into sites of tooth loss in adult mice, the bioteeth erupted and grew, and occlusion of the regenerated teeth was established with hardness comparable to that of natural teeth (***Fig. 1***, top). Further, the tissue structure of the regenerated teeth was similar to that of natural teeth, and a fully matured periodontal ligament structure was also observed, including alveolar bone. The periodontal ligament of the regenerated teeth was shown to retain the physiological capacity to remodel surrounding alveolar bone in response to experimental orthodontic force and to move teeth in a similar manner to natural teeth. In addition, similarly to natural teeth, the dental pulp and periodontal ligament of the regenerated teeth had multiple peripheral nerves, including sympathetic and sensory nerves. Upon application of mechanical stress through dental pulp exposure or dental makeover, upregulation of c-Fos expression in response to intraoral noxious stimuli in some neurons in the spinal trigeminal nucleus was observed for both regenerated and natural teeth, revealing restoration of physiological response to external noxious stimuli in the regenerated teeth. These results demonstrated that not only masticatory function but also the full spectrum of normal tooth physiology could be restored in a tooth regenerated by means of transplantation of bioengineered tooth bud cells, and clearly indicate the clinical applicability of the approach to regenerative therapy against tooth loss [13].

Tooth regeneration using bioengineered tooth units

Elderly people often have severe progressive periodontal disease presenting with extensive destruction of periodontal tissue essential for mastication, and tooth loss has been known to lead to the absorption of surrounding alveolar bone resulting in severe bone defects [14]. For tooth regeneration in the elderly, an approach based on the regeneration of teeth with finished components (*e.g.*, dental prostheses) together with periodontal tissues for immediate functional recovery after implantation would be more appropriate than transplantation of bioengineered tooth germ. On this basis, we developed the "bioengineered tooth unit," which includes tooth and periodontal tissue (*i.e.*, functional unit of tooth), with the aim of developing tooth regeneration technology that allows for immediate functioning.

Because the culture of three-dimensional organs *ex vivo* is not currently possible, we demonstrated our concept by constructing bioengineered tooth units suitable for transplantation by transplanting bioengineered tooth bud

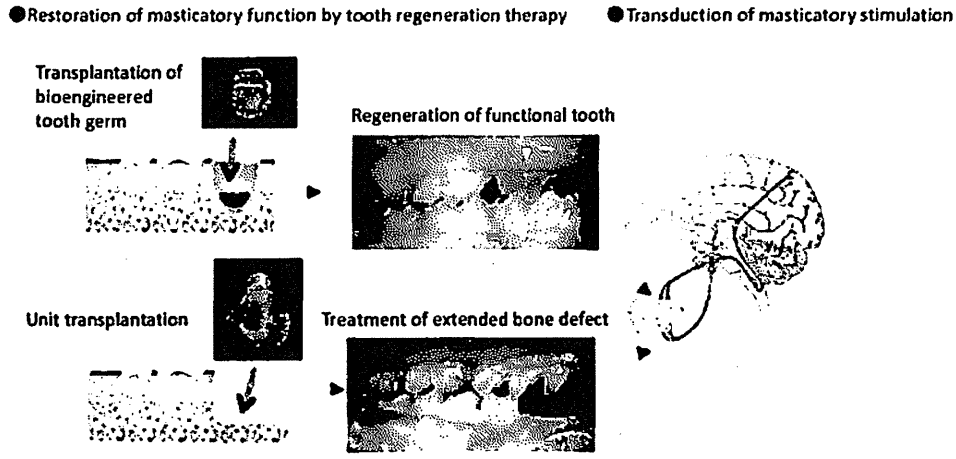

Fig. 1. **Development of tooth regenerative therapy aimed at Anti-Aging.**
Regeneration of functional teeth using bioengineered tooth bud cells and treatment of extended bone defects by bioengineered tooth unit transplantation are expected to aid progress in anti-aging regenerative medicine technologies which enable the transduction of masticatory stimulation to be restored. (Scale bar: 200 μm)